



COMMISSION
OF THE EUROPEAN
COMMUNITIES



FP5- EESD

CREST LEVEL ASSESSMENT OF
COASTAL STRUCTURES BY
FULL-SCALE MONITORING,
NEURAL NETWORK PREDICTION
AND HAZARD ANALYSIS
ON PERMISSIBLE WAVE OVERTOPPING

CLASH

EVK3-CT-2001-00058

R
E
P
O
R
T

D40 Report on conclusions of scale effects

February 2005

A. Kortenhaus
J. Van der Meer
H.F. Burcharth
J. Geeraerts
T. Pullen
D. Ingram
P. Troch

Leichtweiß-Institute for Hydraulics
Germany





COMMISSION
OF THE EUROPEAN
COMMUNITIES



FP5 - EESD

CREST LEVEL ASSESSMENT OF
COASTAL STRUCTURES BY
FULL-SCALE MONITORING,
NEURAL NETWORK PREDICTION
AND HAZARD ANALYSIS
ON PERMISSIBLE WAVE OVERTOPPING

CLASH

EVK3-CT-2001-00058

R
E
P
O
R
T

Workpackage 7

Quantification of
Measurement Errors,
Model and Scale Effects
Related to Wave Overtopping

Version 1.4
February 2005

A. Kortenhaus
J. van der Meer
H.F. Burcharth
J. Geeraerts
T. Pullen
D. Ingram
P. Troch

Contents

List of Figures	iii
List of Tables.....	iv
1 Introduction.....	1
1.1 Motivation	1
1.2 CLASH project	1
1.3 Principal objectives	2
2 Review and theoretical background.....	2
2.1 Definitions	3
2.2 Measurement effects	5
2.3 Model effects	5
2.3.1 Wave generation	6
2.3.2 Influence of wind	7
2.3.3 Other model effects	10
2.3.4 Discussions	11
2.4 Scale effects	13
2.4.1 Introduction	13
2.4.2 Previous investigations	14
2.4.3 Porous flow scale effect	17
2.4.4 Surface flow scale effects	18
2.4.5 Influence of surface tension	20
2.4.6 Influence of kinematic viscosity	22
2.4.7 Summary of scale effects on overtopping	25
3 Description of methodology.....	26
3.1 Measurement uncertainties	28
3.2 Model effects	29
3.3 Scale effects	30
4 Results.....	30
4.1 Samphire Hoe	31
4.2 Zeebrugge rubble mound breakwater	31
4.3 Ostia rock breakwater	33
4.4 Numerical models	34
4.4.1 Amazon code	34
4.4.2 Numerical simulation results of 2D wave overtopping at Ostia breakwater	38
4.5 Correction procedures for model and scale effects	42

4.5.1	Monte Carlo simulation for model effects and uncertainties	42
4.5.2	Method to account for scale effects	46
5	Summary and concluding remarks.....	55
	References.....	56

List of Figures

Fig. 1:	General methodology for analysis of scale effects in CLASH.....	2
Fig. 2:	Overview of possible reasons for differences in prototype and laboratory results.....	3
Fig. 3:	Similitude laws and scale effects in modelling wave loads and response of sea dikes in Führböter (1986)	4
Fig. 4:	Illustration of surface flow and porous flow domains during run-up.....	14
Fig. 5:	Influence of surface tension σ_0 on wave run-up velocities after Schüttrumpf (2001).....	22
Fig. 6:	Influence of kinematic viscosity on wave propagation velocity in shallow water after Schüttrumpf (2001)	23
Fig. 7:	Influence of viscosity on wave run-up and overtopping velocities after Schüttrumpf (2001).....	25
Fig. 8:	Sketch of systematic approach to quantify scale effects in CLASH	27
Fig. 9:	Prototype results, 2D and 3D test results with comparison to Besley formula	31
Fig. 10:	Relative mean overtopping rates from LWI tests plotted against the relative freeboard with comparison to Van der Meer formula and prototype results.....	32
Fig. 11:	Relative mean overtopping discharges from FCFH (3D) and UGent (2D) tests plotted against the relative freeboard with comparison to Van der Meer formula and prototype results	33
Fig. 12:	Computational domain with step porous structure	35
Fig. 13:	The Darcy-Weisbach friction factor plotted against Reynolds number	35
Fig. 14:	Instantaneous dimensionless jet velocities (solid breakwater).....	36
Fig. 15:	Instantaneous overtopping volumes measured on the impermeable structure	37
Fig. 16:	Instantaneous overtopping jet velocity on the impermeable slope.....	37
Fig. 17:	Instantaneous distribution of the Darcy-Weisbach friction factor for varying wave heights on the impermeable structure.....	38
Fig. 18:	Simulation results calculated at times 18.8, 19.2, 19.6, 20.0 and 20.4 s for the 1/20 scale model	40
Fig. 19:	Results and differences of one standard deviation for wave overtopping formula of the Zeebrugge breakwater.....	45
Fig. 20:	Reduction of wave overtopping due to reduction of wave run-up on the seaward slope for the Zeebrugge storm data	48
Fig. 21:	Discharge rates and the effect of the transport factor W_s	49
Fig. 22:	Scaling map for wave overtopping results over coastal structures from small-scale model tests	53
Fig. 23:	Results of the application of the parameter map for scaling to the test case of Zeebrugge	54
Fig. 24:	Results of the application of the parameter map for scaling to the test case of Ostia.....	55

List of Tables

Tab. 1:	Summary of measurement uncertainties.....	5
Tab. 2:	Summary of model effects.....	12
Tab. 3:	Overview of scaling methods.....	13
Tab. 4:	Overview of scale effects for various types of hydraulic models.....	16
Tab. 5:	Previous studies on measurement, model and scale effects for various processes on a rubble mound structure and a sea dike	17
Tab. 6:	Material characteristics for the 1/20 Ostia scale model.....	39
Tab. 7:	Averaged (during one wave period) layer thickness h , the averaged flux (or overtopping rate) q and the averaged Reynolds number Re , taken on the breakwater slope (at the intersection with the SWL) and on the crest (seaward side).....	41
Tab. 8:	Averaged (during one wave period) Reynolds number Re , taken on the breakwater slope (at the intersection with the SWL) and on the crest (seaward side) for the second test conditions.....	42
Tab. 9:	Uncertainties of input parameters and model tests for Monte Carlo simulations regarding wave overtopping (D = deterministic, N = Normal distribution, LN = Log-Normal distribution)	44
Tab. 10:	Results of Monte Carlo simulations of wave overtopping formula with variation of MWL and H_{m0}	45

1 Introduction

1.1 Motivation

Coastal regions in Europe are often densely populated and therefore strongly depend on reliable coastal structures defending them from storm surges, wave attacks and flooding. Due to climate changes and increasing water levels these threads need to be reconsidered and reliable methods are required to design coastal structures and to quantify the hazards caused by possible overtopping over these structures.

Since coastal structures often differ considerably many investigations have been performed to study the crest heights and stability of these structures. The corresponding data and knowledge is spread all over the various research institutions and universities but has never been linked together to form a universal basis for a global design approach.

Furthermore, results of the international European OPTICREST project in De Rouck et al. (2001) have shown that wave run-up on rubble mound breakwaters may be up to 20% higher than run-up in selected and carefully analysed hydraulic model studies which have investigated the same breakwater. It was assumed that a similar behaviour can be expected for wave overtopping so that further research efforts are required (i) to find the reasons for these differences; and (ii) to quantify these effects so that advice can be given on how to manage scale effects on run-up and overtopping.

1.2 CLASH project

The international CLASH project of the European Union (Crest Level Assessment of coastal Structures by full scale monitoring, neural network prediction and Hazard analysis on permissible wave overtopping) under contract no. EVK3-CT-2001-00058 is focussing on wave overtopping for different structures in prototype and in laboratory. The main scientific objectives of CLASH are (i) to solve the problem of possible scale effects for wave overtopping and (ii) to produce a generic prediction method for crest height design or assessment. Therefore, wave overtopping events are measured at three coastal sites in Europe, namely at (i) the Zeebrugge rubble mound breakwater (Belgium), (ii) a rubble mound breakwater protecting a marina in Ostia (Italy) and (iii) a seawall in Samphire Hoe (United Kingdom). Those measured storm events had been simulated by laboratory tests and / or by numerical modelling and had been compared with the actual measured events. This led to conclusions on scale effects and how to deal with these effects. Workpackage 7 of CLASH is aiming at this comparison of full scale measurements with simulation by laboratory scale model tests and numerical modelling.

1.3 Principal objectives

The overall objectives of this report are to quantify scale effects on overtopping considering the influence of different measurement techniques in the labs and the prototype and also taking into account model effects in the labs.

To achieve this goal chapter 2 first defines the various influences resulting in different measurements of wave overtopping over coastal structures in smaller and larger scale. Effects of measurement techniques, model effects and possibly scale effects will significantly contribute to these differences. It then continues by reviewing the existing information dealing with scale effects and provides some theoretical background on both model and scale effects. From this review the needs for the model investigations planned in CLASH are repeated and the methodology for measurements within CLASH is introduced (chapter 3). Chapter 4 describes how this methodology has been applied to the CLASH example sites and summarises the results for these sites.

The general methodology is summarised in Figure 1 where the grey coloured background marks the area covered by this report.

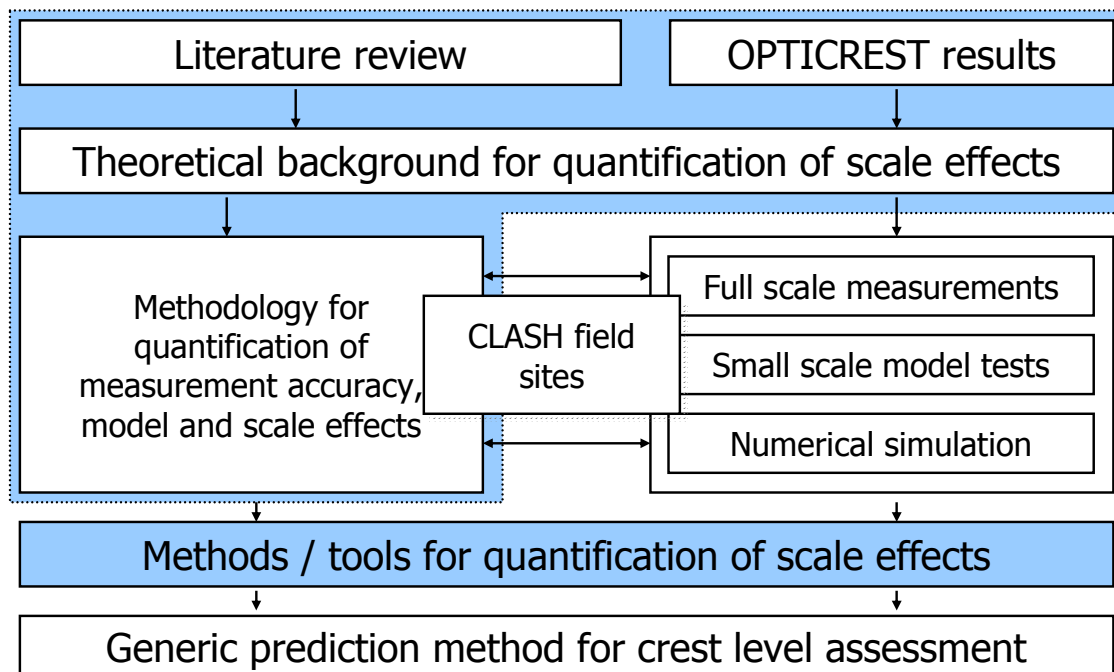


Fig. 1: General methodology for analysis of scale effects in CLASH

2 Review and theoretical background

This chapter reviews reports and papers from the literature which describe previous investigations on scale effects with regard to coastal structures. The information from these findings

will be applied and modified to the overtopping problem which will be followed in CLASH so that an overall theoretical methodology for quantifying scale effects can be derived.

First, definitions of all relevant effects will be given in section 2.1. In section 2.2 a brief summary of some measurement effects will be given. Section 2.3 then collates information regarding model effects as reported in the literature. Special consideration will be given to wind effects. Eventually, section 2.4 deals with scale effects as found in the literature and introduces some theoretical background and critical margins for overtopping investigations of the CLASH structures.

2.1 Definitions

In order to distinguish between the various sources of possible errors when hydraulic model tests are compared to prototype results definitions (Fig. 2) are needed for

- errors resulting from measurement accuracy
- model or laboratory effects
- scale effects

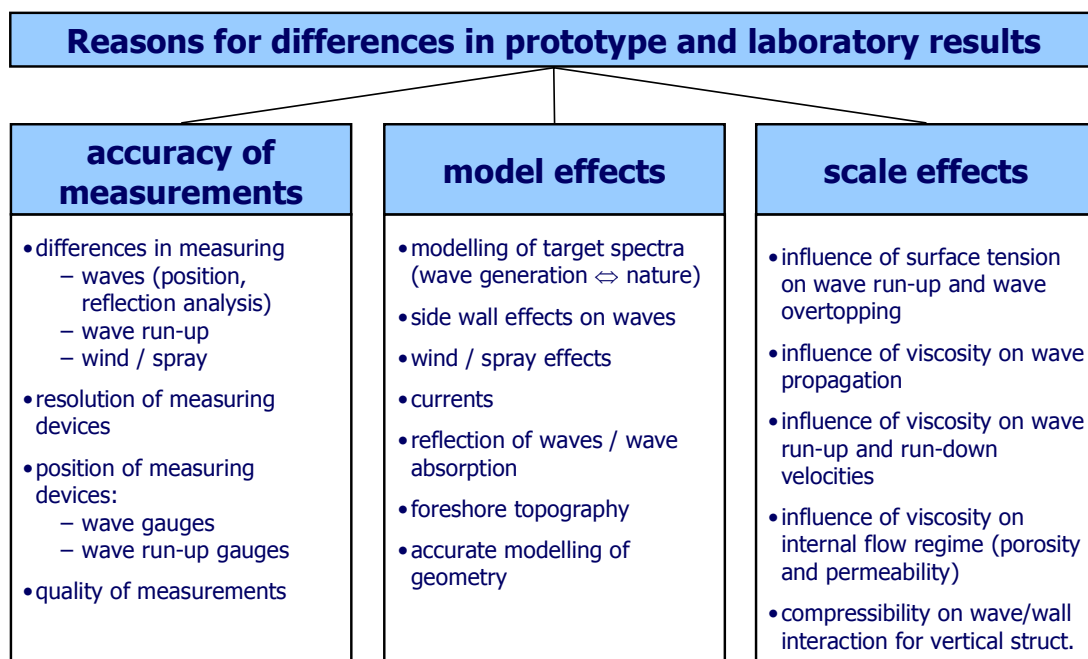


Fig. 2: Overview of possible reasons for differences in prototype and laboratory results

Scale effects result from incorrect reproduction of a prototype water-structure interaction in the scale model. Reliable results can only be expected by fulfilling Froude's and Reynolds' law simultaneously. This is however not possible so that scale effects cannot be avoided when performing scaled model tests, see Oumeraci (1999a) and Oumeraci (1999b).

Since gravity, pressure and inertial forces are the relevant forces for wave motion most models are scaled according to Froude's law. Consequently, friction forces (Reynolds law), elasticity effects (Cauchy law) and surface tension forces (Weber law) are neglected for most models. These forces are principally illustrated for sea dikes in Fig. 3 as described in Führböter (1986) and Oumeraci (1999b). All effects and errors resulting from ignoring the aforementioned forces are called scale effects.

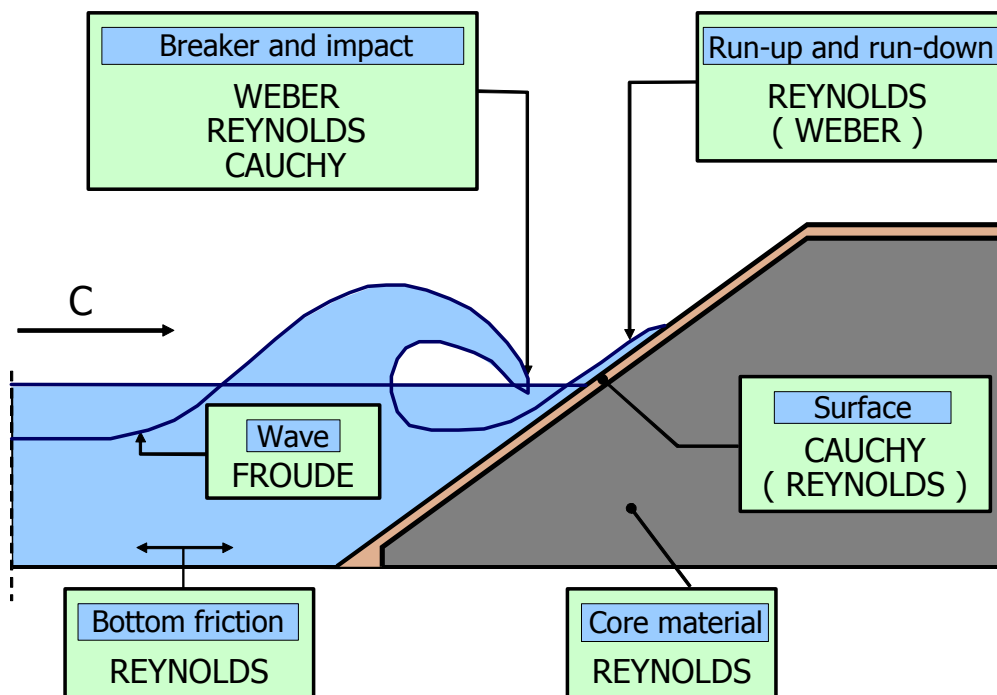


Fig. 3: Similitude laws and scale effects in modelling wave loads and response of sea dikes in Führböter (1986)

Model or laboratory effects originate from the incorrect reproduction of the prototype situation due to inability to model structure, geometry and waves and currents, or due to the boundary conditions of a wave flume (side walls, wave paddle, etc.). Model techniques have developed significantly but still there are influences of model effects on hydraulic model results to be expected. Oumeraci (1999b) pointed out that considerable research efforts are still needed to minimise model effects.

Effects of measurement techniques result from different measurement equipment used for sampling the data in prototype and model situation. These effects which are in the following referred to as “measurement effects” may significantly influence the comparison of results between prototype and model or two identical models. It is therefore essential to quantify the effects and the uncertainty related to the different techniques available.

2.2 Measurement effects

The influence of different measurement techniques or measurement systems on overtopping of a rubble mound breakwater has not yet been investigated. Some results for sea dikes have been found and analysed by Murphy (1999) in the OPTICREST project. However, no model is yet available to (i) quantify the influence of the type of measurement on overtopping and (ii) give recommendations on the preferred system to use for overtopping measurements. The same holds true for measurements of the wave run-up on the seaward slope of the breakwater.

Very few references regarding measurement effects have yet been found. It is therefore essential for CLASH to derive a measurement programme to enable the quantification of differences due to measurement technologies. The results obtained in the OPTICREST project will be used here and will possibly be developed further. These differences should be distinguished with regard to measurement errors and any systematic errors so that upper and lower boundaries for these measurements can be achieved. The aspects given in Tab. 1 should be analysed in more detail.

Tab. 1: Summary of measurement uncertainties

Measurements	Description	Quantification	Remark
Wave measurement			
repeatability of tests	repetition of tests will lead to different results which need a statistical analysis	statistically	
type of wave gauges	different systems to measure waves should be tested and compared	not performed	
calibration of wave gauges	several calibration runs of wave gauges may give different results	statistically	
position and number of wave gauges			Klopman & Van der Meer (1999)
Overtopping measurements			
width of tray	relative to the armour stones in front of it, possibly not so relevant on smooth slopes	statistically	
position of tray	attachment to the crest of the structure (lateral position)		

The methodology on measurement effects will be given in section 3.1.

2.3 Model effects

A review on model effects has been performed by LWI but only few investigations regarding these effects have been found. This may be due to a mixing of these effects with scale effects so that both influences have not been distinguished in the references reviewed so far. Addi-

tionally, model effects are believed to have less influence on the results as compared to scale effects so that most authors have concentrated on scale effects. However, for small overtopping rates there is a significant effect of the actual positions of the armour units.

2.3.1 Wave generation

The principal sources of dissimilarities in the hydraulic model result from the unwanted generation of higher or lower harmonics in the wave trains, see Oumeraci (1999b). To date some improvements have been derived, see Sand (1985) and Funke & Mansard (1979), by both active wave absorption at the paddle, see Gerdes et al. (1991) and passive wave absorption, see Jamieson & Mansard (1987) at the side walls and the rear slope of the flume but still problems exist in eliminating these model effects. Typical model effects in wave flumes (parasitic waves, wave generation, wave absorption etc.) are also described in Müller (1995).

Model effects of small-scale models of rubble mound breakwaters and sea dikes are mainly due to incorrect modelling of the wave field in the flume. This can either be due to the incorrect modelling of the wave spectra (e.g. theoretical spectrum instead of natural sea state, see influence of the spectral width parameter observed in OPTICREST after De Rouck et al. (2001) or the generation of higher harmonics in the wave flume. Both reasons can only be accounted for by improved wave generation technologies (e.g. generation of natural wave spectra in the flume), quality checks and comparison of the wave spectra in the flume compared to prototype conditions.

Damping of waves by side walls in a flume is minimal but to date has no influence on the results as the reference waves are the incoming waves measured in front of the structure. If the waves in front of the paddle are used as reference then there can be larger deviations from prototype related to the incoming waves at the structure. This is due to sensitivity of the wave kinematics to the bottom topography which is never as in prototype.

Reflection of waves cannot be avoided in model facilities, but can be limited effectively by passive and active absorption techniques except for spurious free long waves stemming from wave groups and resonance oscillations in the facility. Anyway, reflected waves can be analysed and filtered from incoming waves with reasonable accuracy both in time and frequency domains.

Cross-waves in the flumes may be generated, especially when vertical structures are investigated in a flume. Downfalling jets from wave overtopping volumes are never uniform over the flume width and generate cross-waves when re-entering the flume in the near-shore region.

2.3.2 Influence of wind

a) Sloped structures

Within OPTICREST the classical dimensionless overtopping variable $Q = q/[g H_{m0}^3]^{0.5}$ was used to derive an exponential formula using the following dependent variables: R_c/H_{m0} [-], Ir [-], R_c/D_n [-] and U [m/s]. The empirical formula given by Eq. (1) is based on hydraulic model tests on the Zeebrugge rubble mound breakwater and was determined using a Neural Network simulation.

$$Q = \frac{q}{\sqrt{gH_{m0}^3}} = \exp \left[-2.8 - 3.4 \left(\frac{R_c}{H_{m0}} \right) + 1.8(Ir - 4) - 0.9 \left(\frac{R_c}{D_n} - 3 \right) + 0.07(U)^{1.5} \right] \quad (1)$$

where q [$m^3/m \cdot s$] is the mean overtopping discharge per meter of crest and per second, g [m/s^2] is the gravity acceleration, H_{m0} [m] is the height of the wave in deep water, R_c [m] is the crest freeboard in reference to the MWL measured in a predefined position in the wave flume, Ir [-] is the Iribarren number, D_n [m] is the nominal diameter of the elements ($D_n = 2180$ mm), and U [m/s] is the dimensional nominal wind speed used in the laboratory experiments.

Differences between the various wind speeds as compared to no wind ($v = 0$ m/s) can mathematically be derived from Eq. (1) for the relative overtopping discharge as follows:

$$f_U = \exp \left[0.07(U)^{1.5} \right] \quad [-] \quad (2)$$

where f_U is the factor of wind influence for the wind speed U [-] and U is the wind speed in the model as above [m/s]. Eq. (2) yields $f_U = 1.4$ for $U = 3$ m/s to $f_U = 3.7$ for $U = 7$ m/s and shows that the influence of wind in this formula is significantly lower than one order of magnitude. Furthermore, it is surprising that the influence of wind seems to remain constant for all wave overtopping discharges whereas it could have been expected that the influence of wind is less important for high overtopping rates.

The latter problem does not occur when the suggestion by SPM (1984) is used where all overtopping rates are multiplied by a factor k' which is dependent on the slope of the structure, the freeboard and the run-up height, thus leading to higher factors for lower wave overtopping rates. The formula does suggest values which are usually in the range of 1.0 to 1.55, therefore suggesting that the maximum increase of wave overtopping is in the range of 55%. This seems rather low in comparison to Eq. (2) and will be more or less negligible for usual variations of wave overtopping discharges. More details on this formula can also be found in González-Escrivá & Medina (2004).

Ward et al. (1994) and Ward et al. (1996) have investigated the influence of wind on wave run-up and overtopping. They found that there is hardly any increase in wave run-up for winds up to 6.5 m/s (less than 10%) on different smooth and rough slopes tested (1:1.5; 1:3 and 1:5). More significant influence can be found for wind speeds of 12 m/s and 16 m/s where

the key process for increasing run-up seems to be the increased wave height H_s at the toe of the structure. For steep rough slopes (1:1.5) additional wind effects have been observed for wind speeds larger than 12 m/s leading to an increase of wave run-up heights up to a factor of 2.0.

For wave overtopping similar results were obtained: wind speeds of 6.5 m/s only have negligible effects on wave overtopping whereas stronger winds of 12 m/s and 16 m/s both increase the wave height and the set-up in front of the structure and therefore the wave overtopping. Factors for wave overtopping may increase up to one or two orders of magnitude for these strong winds. However, the scaling law of wind remains unsolved whereas several processes are discussed which may lead to the increase of wave run-up and overtopping (change of wave height, change of breaker type, support in pushing the waves to run-up, decrease the effect of downwash, advection of splash and spray).

Medina (1998) indicated from Neural Network investigations that only wind speeds larger than 8.0 m/s in the lab had some slight influence on wave overtopping. This result was in line with the results reported from Ward et al. (1996) whereas differences were found in wave overtopping suggesting that there is a stronger effect on wave overtopping also for lower wind speeds. Both these results were however concluded from the behaviour of the Neural Network prediction and were not quantified or verified against individual tests.

González-Escrivá et al. (2002) have investigated the influence of wind on wave run-up and overtopping for the Zeebrugge breakwater. They found a negligible increase for wave run-up in the range of 5% only. More significant influence of wind for wave overtopping has been found also for lower overtopping rates up to one order of magnitude. The formula derived in Eq. (2) is based on the same data and therefore represents the average factors for different wind speeds. It should be noted that some significant wave set-up was also observed in the tests which increased with the wind speed and seemed to have reached up to 10-15% of the water depth in the flume. There is however no conclusion on how much the wave set-up has influenced the overtopping discharges.

b) Vertical structures

Wave overtopping over vertical coastal structures is generally associated with wind, and its effects have been discussed by Ward et al. (1996) and De Waal et al. (1996). Wind may cause overtopping of part of the breaker spray that would otherwise have fallen back into the sea in a situation without wind. It may cause the breaker type to change by deforming the incident wave, or it may cause overtopping by spray generated by the wind on the sea. These are general effects that may not always be pertinent when discussing overtopping at vertical structures. In this case the significant point is whether the overtopping discharge passes over the crest of the structure or falls directly back into the sea. This particular effect is a well known phenomenon that has been discussed by De Waal et al. (1996) and has been observed during the model tests of Samphire Hoe within CLASH.

The majority of investigations into wave overtopping have involved laboratory studies in still air conditions without any consideration of the effect of wind transport. This is due to the considerable scaling difficulties of simulating this effect directly. Three different scaling parameters are required to model the whole system, as summarised below.

- **Froude:** The wave flume is an open channel and is scaled by the Froude number as gravity effects cannot be neglected.
- **Weber:** The process of “green-water” breakup to spray is heavily influenced by surface tension and is therefore Weber scaled.
- **Reynolds:** The transport of (splash and) spray by wind is governed by form drag and is therefore scaled by Reynolds number.

Scaling wind remains a difficult task, especially with regard to its effect on air / spray mixtures, where surface tension, viscosity and droplet size are the same for both prototype and model. Moreover, spray trajectories will be turbulent and should therefore be modelled using Reynold’s scaling, which is incompatible with Froude scaling. Froude law is applied to physical models where gravity is the predominant factor in the fluid motion. Despite the scaling difficulties several attempts have been made to simulate wind effect directly in the laboratory. Experiments have employed various methods to overcome the scaling difficulties, with differing degrees of success. While these tests failed to produce a fully reliable method of predicting the wind effect, they do have a qualitative worth for predicting the magnitude of the wind effect and indicating the threshold at which spray transport by wind may occur.

Recognising the inherent difficulties involved in attempting to scale the effects of wind, De Waal et al. (1996) adopted a novel approach to the problem. It was felt that the most important factor for designers was the maximum effect of wind on overtopping. This could be determined by ensuring that all the discharge that rose over the crest of the structure was collected in the overtopping tank. This process is a simplified simulation of the wind carrying all the spray from overtopping events over the seawall. They constructed a paddle wheel that sat above the crest of the structure, and was rotated at a predetermined speed. Thusly, the discharges were translated to the leeward side of the crest and deposited into the overtopping tank. It was observed during the tests that the paddle wheel transported approximately 90% of the discharge into the collection tank. Using this method no change on the approaching waves was effected, and so there was no change of breaker type or spray generated by wind. This introduces error into the analysis since these effects are neglected, but it nonetheless introduces a significant advance in quantifying the effect that wind has on causing discharges to pass over the crest.

To describe the effect of the paddle de De Waal et al. (1996) defined the Spray Transport Factor (W_s) to quantify the effect on overtopping where W_s is simply the ratio of the transport without wind and the transport with. They discovered that the paddle wheel typically increased overtopping by 30% to 40%, with a maximum of approximately 300%. Davey (2004) revisited the work of de De Waal et al. (1996), and again demonstrated the validity of the paddle wheel method for simulating spray transport. Davey was unable to perform tests with and without the paddle due to time constraints, and compared the paddle results to the empiri-

cal prediction from Besley (1999) for a plain vertical wall. These results are in agreement with de De Waal et al. (1996), with values of W_s generally of the same magnitude.

Recognising the difficulties posed by attempting to simulate the effects of the wind in the laboratory, Pullen & Allsop (2004) chose to study the effects of wind by placing four large fans directly in front of and above the crest. The reason for placing them above the crest was to ensure that they did not effect the incident waves, but rather they assisted in “pushing” the overtopping discharge over the parapet wall in a manner analogous to the paddle wheel used by de De Waal et al. (1996) and Davey (2004). Moreover, these tests were carried out at a scale of 1:20 in 3d, where the use of paddle wheels would not have been practicable. Pullen & Allsop (2004) were able to test each of the conditions with and without wind, in much the same way that De Waal et al. (1996) did with their paddle experiments.

2.3.3 Other model effects

During the OPTICREST project the following observations, which had influences of the test results at LWI, were made by De Rouck et al. (2000):

- **Porosity of armour layer:** Antifer cubes of the lower armour layer were regularly arranged; in comparison to the model the porosity of the prototype can get lower due to subsidence; after filling up the gaps in the model higher values of $Ru_{2\%}/H_{m0}$ were measured;
- **Influence of currents:** After generating currents in front of the structure (AAU) higher dimensionless wave run-up heights due to increasing current velocities were measured; in prototype measurements the strongest currents occur at highest water level whereas the current velocity is nearly zero at mean water level; comparing with the results at AAU the highest wave run-ups have occurred for the highest water level. This result does not agree with the observations from prototype where the run-up increases with decreasing water level and decreasing current velocity;
- **Construction of core:** the core of the prototype, which is partly filled with sand, was rebuilt in the model using a distorted scale according to Burcharth et al. (1999). The sand was washed away during the tests and as a result of this a higher porosity and as a consequence lower wave run-ups can occur;
- **Foreshore topography:** different topographies of the foreshore were constructed at FHFC and UVPLC; but despite a very accurate construction of the foreshore the results of the model tests did not get any closer to the prototype measurements over more simple foreshores.

Due to investigations of Kortenhuis et al. (2004a) the following conclusions were made referring to measurement uncertainties and model effects:

- **Repeatability of tests:** wave parameters (H_{m0} , T_p , $T_{m-1,0}$) fit very well both in the LWI and the UPVLC flume (Coefficient of variations, $CoV \sim 3\%$); concerning to the wave

overtopping the differences at LWI were higher (CoV~13%) than at UPVLC (CoV~10%);

- **Different time windows:** different time windows for wave analysis and different types of wave generation methods had no influence on the estimated wave parameters (CoV~3%);
- **Number of generated waves:** the number of waves in the flume has an influence on the wave overtopping; comparison of 200 compared to 1000 generated waves show differences in overtopping rates up to a value of 20%;
- **Position of the overtopping tray:** the position of the tray at the side of the flume showed also differences in overtopping rates (CoV~20%) from results where the tray was located at the centre of the crest; either it is because of the different arrangement of the Antifer Cubes in front of the overtopping tray or due to the influence of the side walls of the flume;

More differences and their quantifications are given in Kortenhaus et al. (2004a) and Tab. 2. Comparing the first phase of the model tests at LWI with the second phase of model tests the following observations were made:

- **Precision of water level adjustment:** the water level has a large influence on the overtopping results and observations have shown that this is a critical parameter to adjust especially for low overtopping rates;
- **Placement of Antifer cubes:** the varying placement of Antifer cubes results in different overtopping rates at almost every point of the breakwater (model and prototype). Therefore the armour layer in front of the tray has a great influence on the overtopping rate;
- **Lower armour layer:** the lower armour layer for the Zeebrugge case has an influence on the layout of the upper armour layer; despite sufficient knowledge of the upper armour layer layout it has not been possible to arrange the Antifer cubes of the upper layer correctly;

2.3.4 Discussions

Relatively little detailed investigations have been performed yet regarding model effects for small-scale hydraulic models. The aforementioned information is not complete yet and has therefore been amended and is summarised in Tab. 2.

Tab. 2: Summary of model effects

Model effect	Description	Quantification	Remark
Waves			
higher or lower harmonics	generated by insufficient wave generation techniques (soft- and hardware)		can be improved by better wave generation, dissipation
long waves	unwanted long waves in the flume may generate higher water levels temporarily so that wave overtopping is increased	only accounted for in the case of Petten	
number of waves	statistical analysis of waves require at least 1000 waves per test		Should be at least 1000 waves per test
breaking reproduction	is the breaking reproduced correctly in the model		
reproduction of spectra	natural spectra from the field should be reproduced as accurately as possible, sometimes iteration procedures are required to match the field measurements	comparison of wave spectra in the field and the flume	
spectral width	directly related to the previous point	comparison of spectral width is a measure for the quality of reproduction	
Structure geometry and sea bed topography			
3D location	most relevant if layout of structure cannot be reproduced by flume tests		
changes of bed profile during storms	change of bed profile might change the character of waves at the toe of the structure	not accounted for in this project	
armour stone placement	can be very difficult when insufficient information is available, upper layers may depend on lower ones	by re-constructing the same model several times	
reproduction of roughness, porosity and permeability	needs to be done as accurately as possible		
Analysis Methods			
time windows	different time windows in analysis of waves and overtopping	various analysis runs with identical tests	
Wind			
influence of wind	could either influence wave parameters at the toe or 'push' the water over the defence	model tests with and without wind	scaling of wind velocities remains unsolved

2.4 Scale effects

2.4.1 Introduction

An overview of the **scaling models** by Froude, Cauchy, Weber and Reynolds as defined in Fig. 3 are given in Table 3. For the most relevant parameters used in the models the scaling law is derived to calculate N_{measure} defined as ratio of prototype to model measure.

Tab. 3: Overview of scaling methods

Parameter	Froude	Cauchy	Weber	Reynolds
Force ratio	Inertia / Gravity	Inertia / Elasticity	Inertia / Surface tension	Inertia / Viscosity
Equations	$\frac{u}{\sqrt{g \cdot L}} = \text{const.}$	$\frac{\rho \cdot u^2}{K} = \text{const.}$	$\frac{\rho \cdot L \cdot u^2}{\chi} = \text{const.}$	$\frac{u \cdot L}{\nu} = \text{const.}$
Length [m]	N_L	N_L	N_L	N_L
Area [m²]	$N_A = N_L^2$	$N_A = N_L^2$	$N_A = N_L^2$	$N_A = N_L^2$
Volume [m³]	$N_V = N_L^3$	$N_V = N_L^3$	$N_V = N_L^3$	$N_V = N_L^3$
Time [s]	$N_t = \sqrt{N_L}$	$N_t = \sqrt{\frac{N_\rho}{N_K}} \cdot N_L$	$N_t = \sqrt{\frac{N_\rho}{N_\chi}} \cdot N_L^{1.5}$	$N_t = \frac{N_L^2}{N_V}$
Velocity [m/s]	$N_u = \sqrt{N_L}$	$N_u = \sqrt{\frac{N_K}{N_\rho}}$	$N_u = \sqrt{\frac{N_\chi}{N_\rho \cdot N_L}}$	$N_u = \frac{N_V}{N_L}$
Acceleration [m/s²]	$N_a = 1$	$N_a = \frac{N_K}{N_\rho \cdot N_L}$	$N_a = \frac{N_\delta}{N_\rho \cdot N_L^2}$	$N_a = \frac{N_V^2}{N_L^3}$
Mass [kg]	$N_m = N_\rho \cdot N_L^3$	$N_m = N_\rho \cdot N_L^3$	$N_m = N_\rho \cdot N_L^3$	$N_m = N_\rho \cdot N_L^3$
Pressure [Pa]	$N_p = N_\rho \cdot N_L$	$N_p = N_K$	$N_p = \frac{N_\chi}{N_L}$	$N_p = N_\rho \cdot \frac{N_V^2}{N_L^2}$
Force [N]	$N_F = N_\rho \cdot N_L^3$	$N_F = N_K \cdot N_L^2$	$N_F = N_\chi \cdot N_L$	$N_F = N_\rho \cdot N_V^2$
Overtopping rate [l/(s·m)]	$N_q = N_L^{1.5}$	$N_q = \sqrt{\frac{N_K}{N_\rho}} \cdot N_L$	$N_q = \sqrt{\frac{N_\chi}{N_\rho}} \cdot N_L$	$N_q = N_V$

Notes: N is defined as the scaling ratio of prototype and model measure, e.g. $N_L = L_p/L_m$ or $N_F = F_p/F_m$
 ν is the kinematic viscosity of the fluid in [m²/s]; ρ is the density of the fluid in [t/m³]; K is the compressibility of the fluid [t/(m·s²); g is the gravitational acceleration in [m/s²]; χ is the surface tension of the fluid in [kN/m]

A consequence of Froude-scaling of wave dominated hydraulic models is disproportion of viscosity and surface tension.

The flow domain related to the action of incoming waves on a sloping porous structure changes in space and time. During the run-up phase the flow domain can be separated into a jet like surface flow domain and a porous flow domain (Fig. 4).

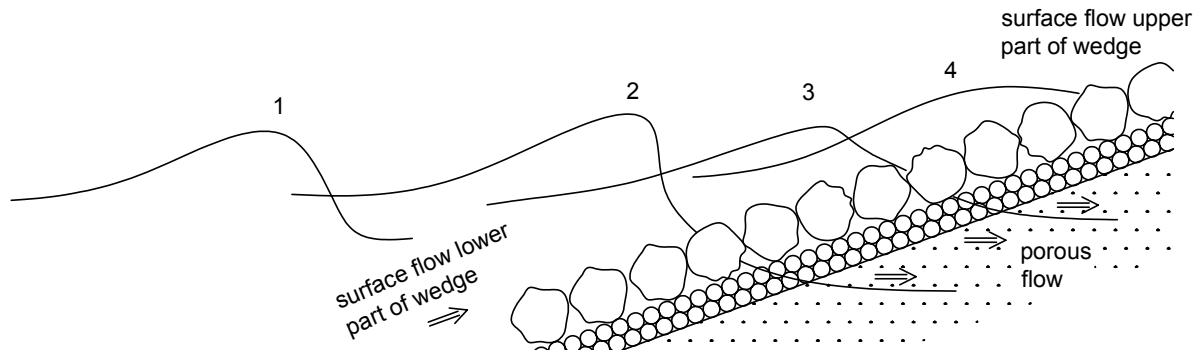


Fig. 4: Illustration of surface flow and porous flow domains during run-up

Froude-scaling, which implies linear length scaling of material diameter has different influences on scale effects in the two domains. Besides viscosity also surface tension and wind may cause scale effects in Froude scale models. These effects are discussed in the following.

2.4.2 Previous investigations

The influence of **surface tension** on wave propagation has first been investigated by Le Mehauté (1976). He proposed critical water levels not lower than 2 cm and critical wave periods not lower than 0.35 s. This can be proved theoretically by determination of the wave celerity, see Oumeraci (1984). Lower values lead to dampening of the waves.

The influence of **kinematic viscosity** on wave run-up and wave overtopping increases with decreasing flow velocity, so in case of small overtopping rates (small layer thicknesses) the turbulent boundary layer does no longer exist, see Schüttrumpf (2001). This means increasing hydraulic resistance on the slope and thus relatively higher energy losses. This behaviour has been verified by test results in different model scales. Small-scale model investigations have shown lower wave run-up heights (Van der Meer (2004); Klein-Breteler & Pilarczyk (1996); Schulz (1992)) and lower overtopping rates (Kajima & Sakakiyama (1994) as compared to large-scale model investigations. Further prototype and model tests by Sakakiyama & Kajima (1998) for a seawall covered with armour stones have indicated that Reynolds numbers in the model should not be lower than $Re_{crit} = 10^5$. Weggel (1976) has shown experimentally that the influence of scale increases for small overtopping rates, which has been explained by viscous effects in the thin run-up layer.

A couple of hydraulic model investigations have been performed in different scales testing for stability of armour layers. Results of Hudson & et al. (1979), Delft Hydraulics (1983), Mol (1983), Torum et al. (1977) were checked for scale effects. The results of these studies on rubble mound breakwaters have not shown any scale effects, Reynolds numbers for the ar-

mour layers in all of these tests were above $3 \cdot 10^4$ (see Oumeraci (1999b)). Earlier tests on rubble mound structures by Hudson & et al. (1979) and Dai & Kamel (1969) suggested much higher values of $4 \cdot 10^5$ (see Sharp & Khader (1984)). Additionally, Kajima & Sakakiyama (1994) summarised model tests with regular waves investigating the scale effects on the stability number. These investigations have proposed correction factors for Reynolds numbers below $3 \cdot 10^5$. Later studies of wave armour layers in front of vertical caisson breakwaters by the same authors still show significant differences for larger deformations and overtopping (larger scale gives larger results). For small deformations the scale effects were negligible. Critical Reynolds numbers or a practical advice for performing model tests are however not given. Oumeraci (1984) and Oumeraci (1998) proposed correction factors to cope with scale effects in stability equations for the armour layer. The critical Reynolds number ($Re_{crit} \approx 3 \cdot 10^4$) was derived from hydraulic model studies described above.

Oumeraci (1999b) has summarised examples and principal sources for scale effects related to different hydraulic models. These examples, the principal sources and further reading are given in Table 4. Scale effects on sediment transport models have been ignored here since they are not relevant for the CLASH project (see Oumeraci (1984) or Oumeraci (1999b) for more details on these models).

Pearson et al. (2002) carried out a series of vertical and near-vertical wall tests in the large wave flume at UPC Barcelona. These large-scale tests were designed to be directly comparable to small-scale tests carried out in Edinburgh. Both test programmes included conditions under which impulsive (violent) overtopping took place. Over a wide range of conditions, large-scale data was found to be in very good agreement with the small-scale data - no scale effect could be measured.

Theoretical investigations on scale effects for sea dikes have been performed by Schüttrumpf (2001). Formulae were developed to estimate the influence of scale effects on the most relevant processes related to sea dikes. These formulae will be introduced and further discussed in the subsequent sections.

As already concluded from results of the OPTICREST project this review showed that the influence of scale effects on the various physical processes in a rubble mound breakwater, on sea dikes and for vertical walls is not yet fully investigated. The advice for influence of the scale effects on the stability of armour stones still differs in the order of one magnitude. Therefore, these influences need to be studied further. The matrix given in Table 5 shows the investigations so far and some of the principal results.

Tab. 4: Overview of scale effects for various types of hydraulic models

	Description	Sources of scale effects	Results	References
wave models	short waves	dissimilarity of bottom friction and wave transmission, surface tension if $T < 0,35$ s or $d < 2$ cm	<ul style="list-style-type: none"> - correction formula for viscous effects by Keulegan (1950) - lower transmitted wave energy, use larger stones than derived from Froude's law - higher reflection from porous structure 	Keulegan (1950); Le Mehauté (1976); Hughes (1993); Burcharth et al. (1999)
	long waves	as for short waves, even more pronounced in undistorted models	<ul style="list-style-type: none"> - larger reflection from distorted models - for wave transmission see above - wave dissipation is similar if $d_{\max} = 0.06 \cdot T^2 / (N_h/N_L)^2$ with d_{\max} in [m] and T in [s]; N_h is the height factor in distorted models 	Le Mehauté (1976); Hudson & et al. (1979)
structure models	rubble mound breakwaters	frequent scale 1:50, thus dissimilarity of viscous forces	<ul style="list-style-type: none"> - critical Reynolds numbers for stability of the armour layer in the range of $3 \cdot 10^4$ - nomogram by Jensen & Klinting (1983) for distortion of permeability (core) - method by Burcharth et al. (1999) for the pore pressures and grain sizes in the breakwater core 	Dai & Kamel (1969); Torum et al. (1977); Hudson & et al. (1979); Broderick & Ahrens (1982); Jensen & Klinting (1983); Mol (1983); De Rouck et al. (2001) Burcharth et al. (1999)
	sea dikes	dissimilarity in breaker index and consequently in wave energy dissipation, effect of air entrapment/entrainment for impact pressures	<ul style="list-style-type: none"> - run-up heights smaller than in prototype (15% to 25% due to breaker index) - run-up velocities have been observed larger and smaller than in prototype - critical Reynolds number for wave overtopping about 10^3 after Schüttrumpf (2001) - impact pressures can be much higher in model for steeper slopes than 1:4 ($Re < 3 \cdot 10^5$) 	Schulz (1992); Popov & Ryabych (1971); Schüttrumpf (2001)
	vertical breakwaters	dissimilarity in waves breaking at the structure; air entrapment / entrainment, no information on overtopping	<ul style="list-style-type: none"> - impact pressures in model can be much higher than in prototype - impacts are usually relatively shorter in model than in nature - correction method by Kortenhuis & Oumeraci (1999) - no differences in wave overtopping behaviour for vertical walls 	Oumeraci et al. (2001); Kortenhuis & Oumeraci (1999) Pearson et al. (2002)

Tab. 5: Previous studies on measurement, model and scale effects for various processes on a rubble mound structure and a sea dike

	Relevant model	Surface tension		Kinematic viscosity	
		Authors	Results	Authors	Results
Wave propagation	Fr, Re, We	Le Mehauté (1976)	$d < 2\text{cm}$ $T < 0.35\text{ s}$	Biesel (1949); Schüttrumpf (2001)	usually no influence
Wave breaking	Fr, Re, We	Miller (1972)	higher breaking waves with lower surface tension		
Run-up velocities	Fr, Re, We	Schulz (1992); Schüttrumpf (2001)	higher velocities if surface tension is higher	Schulz (1992)	higher importance for lower velocities, higher velocities in larger scale
Run-up height	Fr, Re, We			Schulz (1992); Klein-Breteler & Pilarczyk (1996); Van der Meer (2004)	higher run-up heights in larger scale
Overtopping	Fr, Re, We			Weggel (1976); Kajima & Sakakiyama (1994); Schüttrumpf (2001); Sakakiyama & Kajima (1998)	higher overtopping in larger scale or prototype $Re_{crit} = 1 \cdot 10^5$
Stability armour	Fr, Re			Sakakiyama & Kajima (1998); Oumeraci (1998)	various critical Reynolds numbers $Re_{crit} = 3 \cdot 10^4$
Velocities core	Fr, Re			Burcharth et al. (1999)	relatively larger stone size in smaller scale

Fr = Froude's law; Re = Reynolds' law; We = Weber's law

The theoretical background of the aforementioned investigations is highlighted in the following section to be able to derive some recommendations for scale models to avoid scale effects.

2.4.3 Porous flow scale effect

The prototype porous flow will in conventional structures be rough turbulent in the filter layers and in most of the core. This is not the case in small-scale models the size of which can be characterized by significant wave heights in the range $H_s = 0.05 - 0.30\text{ m}$, filter grain diameters in the range $0.01 - 0.03\text{ m}$ and core material diameters of $0.001 - 0.003\text{ m}$, if scaled linearly. The flow in the core and in the filter layers will not be rough turbulent except for the

largest models for which only limited parts of the filters and the core can have this type of flow, however only for a fraction of the wave period.

The consequence of this is that kinematic similarity between flow in prototype and model cannot exist, as the flow resistance will be relatively too large and velocities too small in the model. This will affect the surface flow as less water penetrates into the porous structure leaving a larger proportion of the incoming water to remain on the surface. The consequence is higher run-up and more overtopping water. Compensation for this blocking effect can be dealt with by enlarging the grain sizes, for example as proposed by Burcharth et al. (1999).

If in the prototype the core is completely saturated during wave action then the model core grain size has no influence on overtopping as long as the model core is also saturated. Moreover, for flatter slopes with relatively thick armour and filter layers there will only be a small influence of core permeability on the overtopping discharge.

2.4.4 Surface flow scale effects

The character of the surface flow changes considerably in space and time during run-up. Where and when the thickness of the run-up wedge is several times the roughness of the armour units, the flow has sectionwise similarities with the bottom part of flow in a wide rectangular conduct. But when and where the wedge thickness is less than the roughness, as is the case in the upper part of the run-up wedge, the flow has similarities to flow around obstacles. Details of this analyses and considerations are taken from Burcharth (2004) and are summarised in the following sections.

a) Flow in lower part of run-up wedge

In order to avoid viscous scale effects in Froude models it is a necessity that the type of flow is similar to that in prototype. For the surface flow it means that the flow must be rough turbulent. For flow in pipelines the criterion is that the von Karman number

$$K = 0.3 \frac{U_F k}{\nu} > 10 - 40, \quad (3)$$

where U_F is the friction velocity, k is the roughness and ν the kinematic viscosity.

U_F can be estimated from

$$\frac{U}{U_F} = 6.4 + 2.45 \ln \frac{R}{k}, \quad (4)$$

where U is the average flow velocity and R is the hydraulic radius, here set equal to the depth of water over the rough surface. As the range of R/k in the lower part of the run-up wedge is 3 - 10 then $U_F = 10$, approximately.

Typical prototype values are $U = 2 - 7$ m/s, $U_F = \text{app. } 0.2 - 0.7$ m/s and $k = 0.5 - 2.0$ m. This gives the following range: $K = 3 \cdot 10^4 - 140 \cdot 10^4$.

In model scale 1:50 the values are $U = 0.28 - 0.99$ m/s, $U_F = \text{app. } 0.03 - 0.1$ m/s and $k = 0.01 - 0.04$ m. This gives $K = 90 - 1200 > 10 - 40$.

Consequently it seems reasonable to assume that the flow in the lower part of the run-up wedge is rough turbulent as in prototype.

This conclusion is in agreement with Kamphuis (1975) who, based on wave friction factor considerations suggested the following criterion for the lower limit of rough turbulent oscillatory flow

$$\text{Re} = \frac{U_{\max} \cdot a}{\nu} \geq 200 \frac{a}{k_s} \sqrt{\frac{f_w}{2}} \quad (5)$$

with

$$f_w = \frac{2}{5} \left(\frac{a}{k_s} \right)^{-3/4} \text{ for } \frac{a}{k_s} \leq 100 \quad (6)$$

leading to

$$\text{Re} \geq 447 \left(\frac{a}{k_s} \right)^{1.375} \text{ for } \frac{a}{k_s} \leq 100 \quad (7)$$

in which U_{\max} is max velocity in purely oscillatory flow, a is the amplitude in the near bed wave orbital motion, k_s is the Nikuradse grain roughness, and f_w is the wave friction factor after Jonsson (1966).

For a small scale model we can have a/k_s in the range $0.1/0.03 - 1.0/0.02 = 30 - 50$ leading to the condition $\text{Re} \geq 4.8 \cdot 10^4 - 9.7 \cdot 10^4$. This is generally fulfilled.

The flow in the lower part of the run-up wedge is neither a steady flow nor an oscillatory flow as assumed in the approximate analyses given above. However, as they both point to the same conclusion it is trustworthy.

b) Flow in upper part of run-up wedge

The flow resistance in the region of small water depth is dominated by the drag force exerted upon the armour units (inertia forces are of minor importance).

In prototype the Reynolds number, even in the very upper part of the run-up wedge, will be larger than $\text{Re} = u \cdot d / \nu = 0.5 \cdot \frac{1}{10^{-6}} = 5 \cdot 10^5$, u being a characteristic flow velocity, and d a characteristic width of the armour unit.

In a 1:50 scale model the corresponding Reynolds number will be $1.4 \cdot 10^3$. This reduction has a significant influence on the drag coefficient, C_D . Although not the same flow, it is useful to consider the drag coefficients for flow past single cylinders or arrays of cylinders. For circular or rounded cross sections the variation of C_D with Re is large, typically a 50% to 100% increase in C_D when Re is reduced from $5 \cdot 10^5$ to 10^4 . For flat sided objects with sharp corners the increase in C_D is less, but still significant. For objects of short length to width ratio there is a general reduction in the drag coefficients compared to those for cylinders (infinite length to width ratio). Although this reduction factor is smaller for supercritical flow ($Re \geq 10^6$) than for sub critical flow ($Re \leq 10^5$) there is still a difference in C_D for the flow in prototypes and small scale models.

The effect of this is smaller run-up heights and less overtopping in small scale Froude models than in prototypes. This scale effect is much more significant for small overtopping rates than for the larger ones and might explain why sometimes no overtopping occurs in small scale models as opposed to prototype.

2.4.5 Influence of surface tension

The influence of surface tension on **wave propagation** was investigated by Le Mehauté (1976). Based on the extended dispersion equation

$$c^2 = \left(\frac{gL}{2\pi} + \frac{2\pi\sigma_0}{L\rho_w} \right) \tanh\left(\frac{2\pi d}{L} \right) \quad (8)$$

he showed that the surface tension can be disregarded, if the water depth d is larger than 2.0 cm and the wave period T is longer than 0.35 s. These findings have been confirmed by Oumeraci (1984) using shallow water conditions.

Usually the influence of surface tension on **wave breaking** (air entrainment!) as well as on wave run-up, wave run-down and wave overtopping (especially for low layer thicknesses) cannot be ignored. Kolkman (1984) has shown that surface tension on flat slope causes a stop of flow for layer thicknesses below 3.5 mm. Model investigations by Miller (1972) have shown that a reduction of surface tension has induced an increase of breaking waves and a landward shifting of the breaker point. Additionally, based on the high surface tension in the model the air entrainment will decrease and a higher run-up velocity v_A on smooth slopes in the hydraulic model is observed, see Schulz (1992).

Wave breaking on a rubble slope and the front wedge flow past the armour units cause air to be enclosed in the flowing water. Due to surface tension effect relatively more air will be enclosed in prototype flow than in the flow in the model. Also the bubble size will be relatively smaller in the prototypes partly because of the saline water as opposed to the fresh water in the models. The smaller bubbles escape more slowly than the larger bubbles. The total effect of this is that due to differences in relative air contents the average mass density of the

uprushing water is smaller in prototype than in the model – disregarding the difference in mass density of salt and fresh water.

Assuming the impulse of the water approaching the slopes to be correctly scaled in the Froude model the effect of the differences in air entrainment would be higher run-up and thus larger overtopping in the prototype than in a small scale model – provided that the air entrainment process in the model does not involve relatively larger energy dissipation (which seems unlikely).

A reduction in average mass density of say 5% will cause an approximately 5% higher run-up. Although the overtopping water contains more air in the case of prototype structures the volume of solid water will be larger due to the non-linearity between the theoretical run-up level and overtopping volume.

The influence of surface tension σ_0 on **wave run-up velocities** can be estimated using the run-up velocity v_a after Schüttrumpf (2001):

$$v_A = k^* \sqrt{2g R_{u,2\%}} \quad (9)$$

where v_a is the wave run-up velocity in [m/s]; $R_{u,2\%}$ is the wave run-up height in [m] and k^* is a roughness coefficient [-] which is dependent on the Reynolds number. Due to surface tension σ_0 the run-up height $R_{u,2\%}$ increases by $z_\sigma = \sigma_0/(\rho_W g h_A)$ so that Eq. (9) may be rewritten as:

$$v_A = k^* \sqrt{2g \left(R_{u,2\%} + \frac{\sigma_0}{\rho_W g h_A} \right)} \quad (10)$$

where ρ_W is the density of water [t/m^3]; g is the gravitational acceleration [m/s^2]; and h_A is the layer thickness of the wave running up the slope [m]. Eq. (10) describes the run-up velocity under consideration of the viscosity (indirectly assessed by the friction coefficient k^*) and the surface tension σ_0 .

Substitution of $h_A = c_2^* \cdot R_{u,2\%}$ after Schüttrumpf (2001), the Froude number for run-up velocities $Fr_A = v_A/(g \cdot h_A)^{1/2}$, and the Weber number for run-up velocities $We = (v_A^2 \cdot h_A \cdot \rho_W)/\sigma_0$ yields:

$$Fr_A^2 = \frac{2 \cdot We \cdot k^*}{c_2^* \cdot (We - 2k^*)} \quad (11)$$

where c_2^* is independent from the slope of the structure and was derived by Schüttrumpf (2001) from model tests to be 0.216. Assuming that $\sigma_0 = 0.073 \text{ N/m}^2$ for 20°C model tests can be compared to Eq. (11) which is presented in Figure 5 and shows that the influence of surface tension is negligible if $We > 10$.

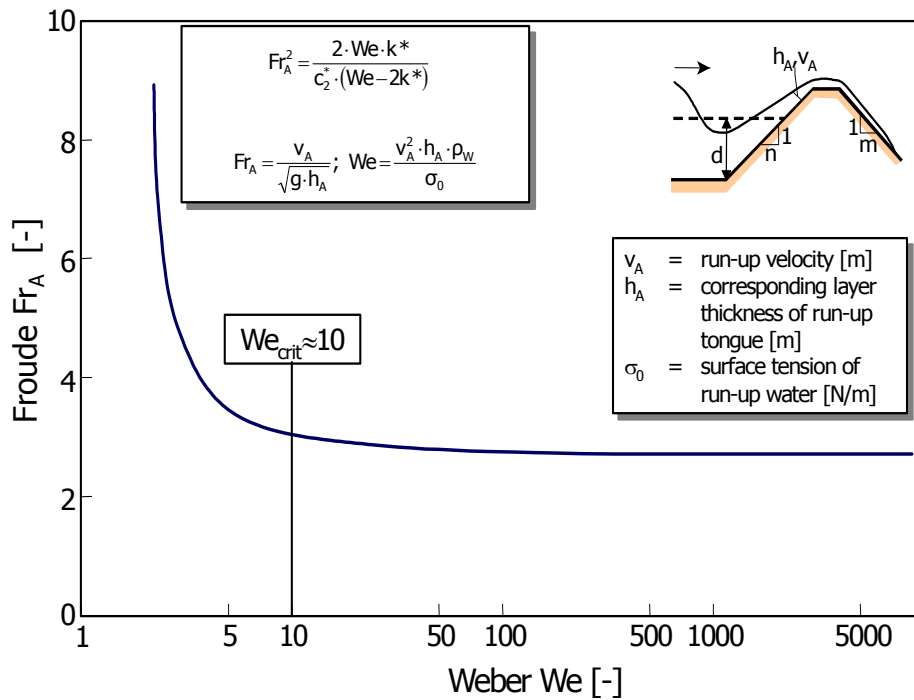


Fig. 5: Influence of surface tension σ_0 on wave run-up velocities after Schüttrumpf (2001)

2.4.6 Influence of kinematic viscosity

In the following the influence of kinematic viscosity on wave propagation, wave run-up and wave overtopping will be investigated.

Biesel (1949) calculated the influence of viscosity ν on the **wave propagation velocity** c on progressive waves as follows:

$$c = \left(1 - \frac{1}{\sinh\left(\frac{4\pi d}{L}\right) \cdot \sqrt[4]{\frac{gL^3}{2\pi^3\nu^2} \tanh\left(\frac{2\pi d}{L}\right)}} \right) \sqrt{\frac{gL}{2\pi} \tanh\left(\frac{2\pi d}{L}\right)} \quad (12)$$

Assuming shallow water conditions ($\sinh(kd) \approx (kd)$) and by using $c^2 = gd$; $kd = (2\pi d/L)$; $Fr_w^2 = c^2/(gd)$ and $Re_w = (cd)/\nu$ Schüttrumpf (2001) arrives at:

$$Fr_w = 1 - \frac{1}{2\sqrt{Re_w \cdot kd}} \quad (13)$$

where k is the wave number defined as $2\pi/L$. Eq. (13) is plotted in Figure 6 for two d/L ratios in shallow water.

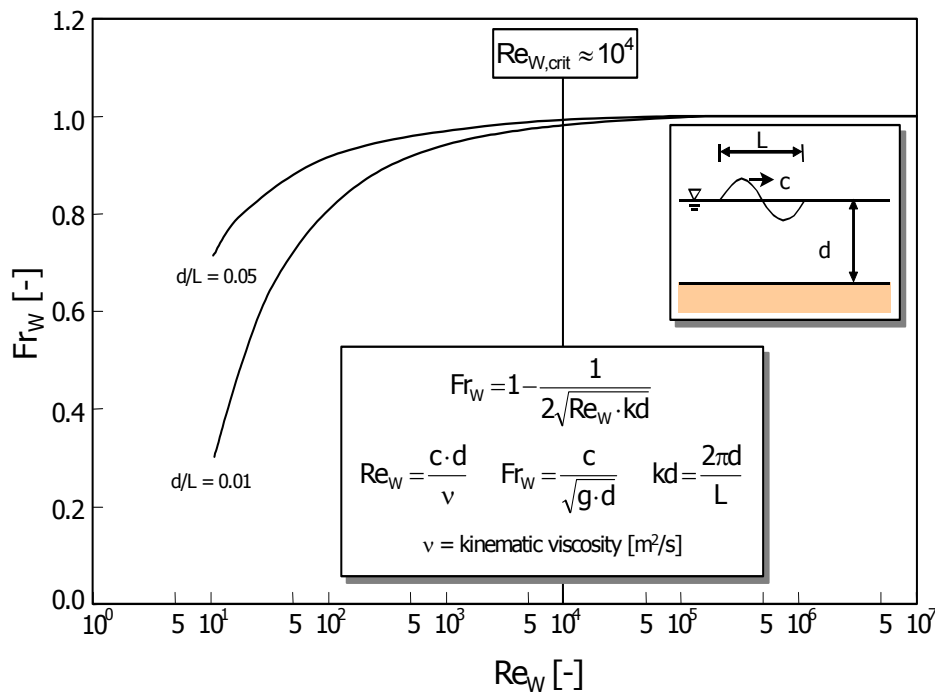


Fig. 6: Influence of kinematic viscosity on wave propagation velocity in shallow water after Schüttrumpf (2001)

Figure 6 shows that a significant influence on the wave propagation only exists for critical Reynolds numbers $Re_{w,crit}$ smaller than 10^4 . The critical Reynolds numbers $Re_{w,crit}$ given by Schüttrumpf (2001) implies water depths of about 2 cm if Eq. (12) is used. This is similar to the minimum water depths for the influence of surface tension on wave propagation. If water depths are larger than 2 cm Figure 6 should be used to verify that Fr_w is not different in between model and prototype results.

The influence of kinematic viscosity on **wave run-up and wave overtopping** can be estimated using the wave run-up velocity of waves on a dike after Schüttrumpf (2001):

$$v_A = k^* \sqrt{2gA} = \sqrt{\frac{1}{(1-\alpha_k)}} \cdot \sqrt{2gA} \quad (14)$$

By transformation and substituting $Fr_q = v_A/(2g \cdot R_{u,2\%})^{0.5}$; $\alpha_k = f \cdot R_{u,2\%} \cdot n/h_A$ (f = friction coefficient; definition is shown in Figure 7); $h_A = c_2 \cdot R_{u,2\%} \cdot n$ it follows:

$$Fr_q = \sqrt{\frac{1}{\left(1 - \frac{f}{c_2}\right)}} \quad (15)$$

Since only an estimation of the threshold of the influence of viscosity on flow conditions is needed here, laminar flow conditions are assumed and the friction coefficient f will be substituted using the Darcy-Weisbach equation.

$$f = \frac{16}{Re} \quad (16)$$

For wave overtopping the flow conditions on the crest of the structure are more important than the wave parameters. Therefore, an overtopping based Reynolds value Re_q will be developed in the following. The Reynolds number is defined as:

$$Re = \frac{v \cdot d}{\nu} \quad (17)$$

where v is the relevant velocity in [m/s]; d is the characteristic length in [m]; and ν is the kinematic viscosity in [m^2/s] which is equal to $1.31 \cdot 10^{-6} m^2/s$ for $10^\circ C$. For the characteristic length d the remaining wave run-up height ($R_{u,2\%} - R_C$) will be used. On the highest point of wave run-up, ($R_{u,2\%} - R_C$) is zero and at still water level ($R_C = 0$) it equals the wave run-up height itself. The remaining average wave run-up velocity is used for v . This means the average velocity of the run-up tongue to the highest point of wave run-up on a virtually extended slope, within half the wave period T can be estimated as follows.

$$v = \frac{R_{u,2\%} - R_C}{0.5 \cdot T} \quad (18)$$

From this velocity and the aforementioned definitions the overtopping based Reynolds number Re_q is derived as:

$$Re_q = \frac{2 (R_{u,2\%} - R_C)^2}{\nu T} \quad (19)$$

Figure 7 shows Eq. (15) and (16) for wave overtopping based Reynolds numbers. The curves in Figure 7 have to be compared to results from model tests where Reynolds numbers are calculated following Eq. (19).

Figure 7 shows that an influence of viscosity on overtopping flow becomes relevant for Reynolds numbers smaller than $Re_{q,crit} = 10^3$. This corresponds to wave overtopping rates when the freeboard height is similar to wave run-up height ($R_C \approx R_{u,2\%}$). Within this range the influence of scale on wave overtopping is relatively high.

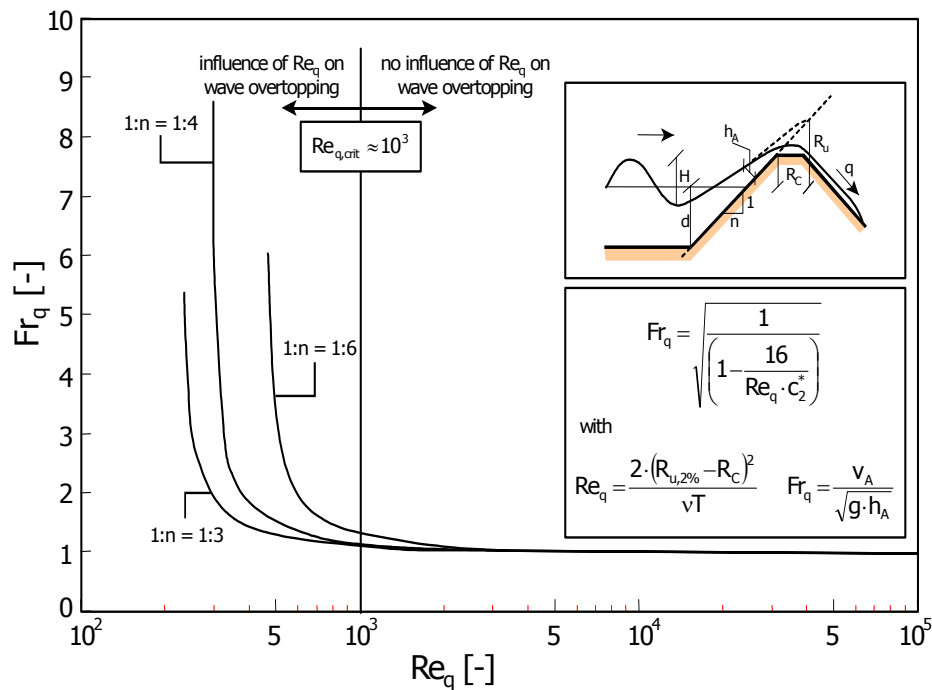


Fig. 7: Influence of viscosity on wave run-up and overtopping velocities after Schüttrumpf (2001)

2.4.7 Summary of scale effects on overtopping

Scale effects related to run-up and overtopping in case of porous rubble slopes in Froude scaled models are qualitatively analysed by considering the porous flow, the surface flow divided in the lower and the upper part of the run-up wedge, and the surface tension effect.

The results can be summarized as follows:

- Froude scaling of porous flow causes too high run-up and overtopping in small-scale models due to viscous effects.
- There seems to be no significant scale effects in the surface flow related to the lower part of the run-up wedge as the flow is rough turbulent both in prototype and small-scale Froude models.
- Significant scale effects - especially for smaller overtopping rates - seems most likely in the flow in the upper part of the run-up wedge as the flow resistance, mainly caused by drag on armour units, is relatively too large in small-scale models due to the increase in drag coefficients with low Reynolds numbers.
- Surface tension scale effect causes relatively smaller air contents in models and thereby a relative increase in mass density leading to too small run-up heights and less overtopping than in prototypes.

The effect of the first item could balance the effect of the last two ones, thus resulting in no observed scale effects on run-up and overtopping.

When compensating the first item by enlarging the grain sizes in the model core then the last two items lead to too small run-up heights and overtopping volumes in a model. The scale effect related to the run-up wedge in the upper part will be relatively larger for smaller overtopping rates.

The first three items have no or marginal relevance to smooth impermeable slopes for which it is also known that scale effects on run-up and overtopping are very small.

The influences of surface tension and viscous effects on wave run-up and overtopping have been also investigated quantitatively. A critical Weber number was determined at $We_{crit} = 10$, viscous effects on wave overtopping become relevant below $Re_{q,crit} = 10^3$. The latter effects lead to increased friction on the slope and consequently to reduced overtopping rates in the model. The same holds true for wave run-up. When using model measurements with wave overtopping based Reynolds numbers smaller than $Re_{q,crit} = 10^3$ those have to be excluded from the analysis. Due to the fact that small Re_q numbers correspond to low wave overtopping rates (for freeboards lower than the wave run-up height), large-scale model tests may be needed for detailed investigation of this range.

It is however not really possible to quantify the discussed scale effects with reasonable accuracy. Consequently some simple rules for scale effect compensation have to be extracted from the comparison of prototype and model data. Therefore, a simple multiplication factor on small-scale model test overtopping/run-up data should contain the following characteristics:

- Should increase with decreasing overtopping rate.
- Should be able to predict overtopping when in the model incorrectly no overtopping occurs due to scale effects.
- Should take into account if the core material grain size has been enlarged to avoid porous flow Reynolds scale effects.

3 Description of methodology

The present literature review related to scaling laws and scale effects (see chapter 2) has shown that there are still considerable gaps in understanding the phenomena leading to scale effects. Quantification of scale effects and practical guidance for scaling necessarily also includes a quantification of the model effects as well as the uncertainties associated with the measurements in the models and in prototype. For this purpose, a systematic approach as sketched in Figure 8 has been proposed for the CLASH project.

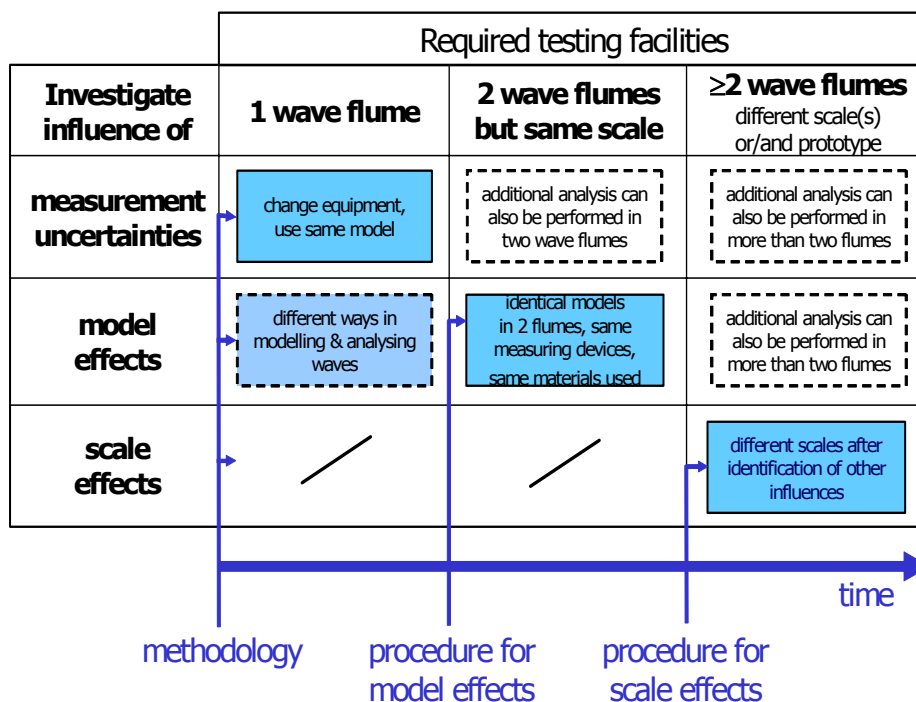


Fig. 8: Sketch of systematic approach to quantify scale effects in CLASH

Figure 8 shows a matrix where the principal sources for differences between prototype and model measurements are listed vertically at the left side (measurement accuracy, model effects and scale effects). On top of the matrix the number of testing facilities needed (wave flumes or field measurement sites) to quantify these effects is listed starting from only one facility to more than two facilities. The idea of the concept is to quantify the aforementioned effects successively, starting with the measurement uncertainties. Usually, the uncertainties associated with the measurements can be assessed in only one flume although it can of course be quantified in several facilities also (see dashed rectangles). The method how this can be achieved will be given in section 3.1.

One or two flumes (the latter with identical scales) will then be needed to quantify model effects. Results from the EU OPTICREST project have shown that results between different flumes where the same model has been tested were comparable and results appeared to be in line for these models. Similar results are therefore expected for CLASH, too. Furthermore, it is essential to quantify effects which may be seen as typical model effects (e.g. theoretical wave spectra instead of natural sea states, reflection compensation of the wave paddle, different ways to model waves, different methods to analyse incoming waves). The latter needs to be performed in two wave flumes, a description of this approach will be given in section 3.2.

The final step in arriving at a method to quantify scale effects is to find differences in measurements when already considering the magnitude of measurement and model effects. These differences have then to be compared to the findings from the literature review and critically discussed. At least two facilities are needed to achieve a quantification of scale effects. These facilities should have a big difference in scale so that any differences in the measurements

cannot be assigned to measurement inaccuracy or other smaller errors. At least one of the ‘facilities’ should be in prototype scale. The theoretical considerations in chapter 2 provide the starting base for this approach but a clear strategy to follow within CLASH has to be drafted in section 3.3.

3.1 Measurement uncertainties

The first step in following the above methodology is to account for and quantify the measurement accuracy of the model tests performed. The following strategy was followed:

Accuracy of the measurement devices: tests were repeated several times after each other where measurement devices of different types (accuracy) and of the same type (repeatability) remained at their positions and all parameters were left identical.

Position and number of measurement devices: this may be important, especially for wave gauges in front of the structures. A high number of wave gauges (distance of $L/16$ with L being the local wave length) to measure the wave field in front of the toe of the structure should be used and then analysed several times with decreasing number of wave gauges. Additionally, the distance of the wave gauges to the side walls in the flume should be tested and any influence should be analysed by a correction factor.

Type of measurement system: this will only be achieved if different measurement techniques are used simultaneously in the same flume. For CLASH, where the key interest is put on overtopping rates, at least three measurement techniques (weighing of overtopping tank, measurement of water level in the tank, pressure transducer at the bottom to measure the height of water in the tank) to measure overtopping volumes should be tested and analysed. This includes direct comparison of these techniques as well as repeatability of tests using one technique only.

Analysis method of tests: they may also result in different results. Therefore, the same tests should be analysed by different analysis methods and software in order to visualise the differences. This applies for wave analysis (time domain analysis, frequency domain analysis, different time frames for analysis), overtopping analysis (different time frames) and general questions such as logging frequency, etc.

The errors found in the measurement techniques should be plotted for overtopping rates and then be compared with respect to systematic errors and random errors. It can be expected that the influence of errors on small overtopping rates is much higher than for high overtopping rates. This can however not yet be quantified. Furthermore, the influence of errors in wave heights, water levels and geometric measures on the overtopping rate should be quantified so that the parameters can be derived which need most careful consideration when constructing a model where overtopping rates are going to be measured.

The following procedure to assess the measurement effects is therefore proposed:

- derive a coefficient of variation (CoV) from test repetitions to account for the uncertainties in measurements;
- derive a second CoV from tests with a high number of wave gauges to account for their spatial variability;
- derive correction factor for distance of wave gauges from the side walls;
- derive a third CoV for test analysis depending on the type of measurements. Furthermore a clear guidance on which system to prefer is needed as a result from these tests;
- derive further coefficients of variation to account for differences in analysis methods. If any systematic errors are analysed correction factors should be proposed to account for these differences;

3.2 Model effects

The next step is to quantify the differences resulting from model effects. Within CLASH the detailed instructions and know-how from the previous OPTICREST project as described in Frigaard & Schlütter (1999) was followed as closely as possible to perform all model tests in an identical way. It is evident that very little can be done in only one wave flume to obtain results on differences due to these model effects. It is therefore desirable to use identical measurement techniques with identical positions of measurement equipment (and an identical model) in two flumes.

Assuming that results from the model are identical or within the range of uncertainty due to the measurement accuracy there might be still model effects when compared to prototype results. These differences may be due to the identical restrictions in the wave flumes compared, such as the presence of side walls or the wave generator or due to the fact that the influence of wind has been ignored during the model tests. Since the main differences between model and prototype results will presumably result from model effects it is impossible to quantify these effects by using prototype results. The following comparison between different

ereich Bauingenieurwesen, Technische Universit#xE4;t
 these model effects: use flumes or wave basin with different widths so that the influence of the side walls plays a different role and see whether there is any difference in the results, compare results using Keulegan model;

- **effect of wave generator:** different wave generators in identical flumes are needed to quantify any differences in the results;
- **effect of wind:** only possible, if one of the flumes does have possibilities to study wind effects (e.g. UPVLC flume);
- **effect of wave set-up:** comparison of 2D wave flume and 3D basin (perpendicular wave attack) is needed to quantify this effect;
- **generation of higher and lower harmonics:** different wave generation software should be used in one flume so that a comparison of the generated wave spectra may give the magnitude of resulting differences;

Results from measurement uncertainties and model effects will then be brought together and analysed within a Monte-Carlo simulation taking into account a mean value, the standard deviation and a typical statistical distribution for each of the aforementioned parameters. This will then be included in a standard formula for wave overtopping to show the magnitude of potential differences if all these values are uncertain.

3.3 Scale effects

The final step in following the above methodology is to quantify scale effects when analysing prototype and model measurements of the CLASH structures. Besides the requirements which are needed to assess the measurement accuracy and the model effects the following details need to be reported from the prototype and model tests:

- description of how the model scale was achieved and what are the magnitudes of resulting water depths and wave parameters;
- detailed description of the construction of rubble mound breakwaters and size distribution of stone material for armour, underlayers and core;
- description of modelling the foreshore in the model.

Based on this information the results from model and prototype measurements for the structures investigated under CLASH will be plotted and a new method to account for possible scale effects will need to be derived.

Furthermore, numerical models will be used to look into the details of scale effects. For this purpose simple identical models with a rough slope have been set up in a numerical model using different scales. Results for numerical overtopping will be compared in these models and tested for scale effects. These results will then be used together with differences from the model and prototype data and a method will be derived to quantify scale effects.

4 Results

This chapter describes the results of prototype and model data from three different sites within CLASH: (i) Samphire Hoe, section 4.1; (ii) Zeebrugge rubble mound breakwater, section 4.2; (iii) Ostia rock breakwater, section 4.3. The description focuses on the comparison of prototype events which have been reproduced in at least two models. Results are discussed in the light of uncertainties and model effects together with possible scale effects. In section 4.4 the results of the numerical analysis of scale effects are described in more detail. Finally, section 4.5 describes and discusses the proposed method to account for model and scale effects.

4.1 Samphire Hoe

Videos have been recorded from the field and the model tests which show very similar behaviour in the water mass being thrown up at the vertical wall. The significant difference seems to be the wind blowing much of the spray beyond the overtopping container.

In Fig. 9 the overtopping results from the prototype at HRW as well as the model tests at UEDIN (2D) and HRW (3D) are plotted together with the overtopping rate against the free-board R_d . The Besley formula from Environment Agency (1999) was also plotted. It should be noted that the 1 May storm data with strong wind effects have been multiplied by a factor of 3.0 to account for the spray blown beyond the overtopping containers.

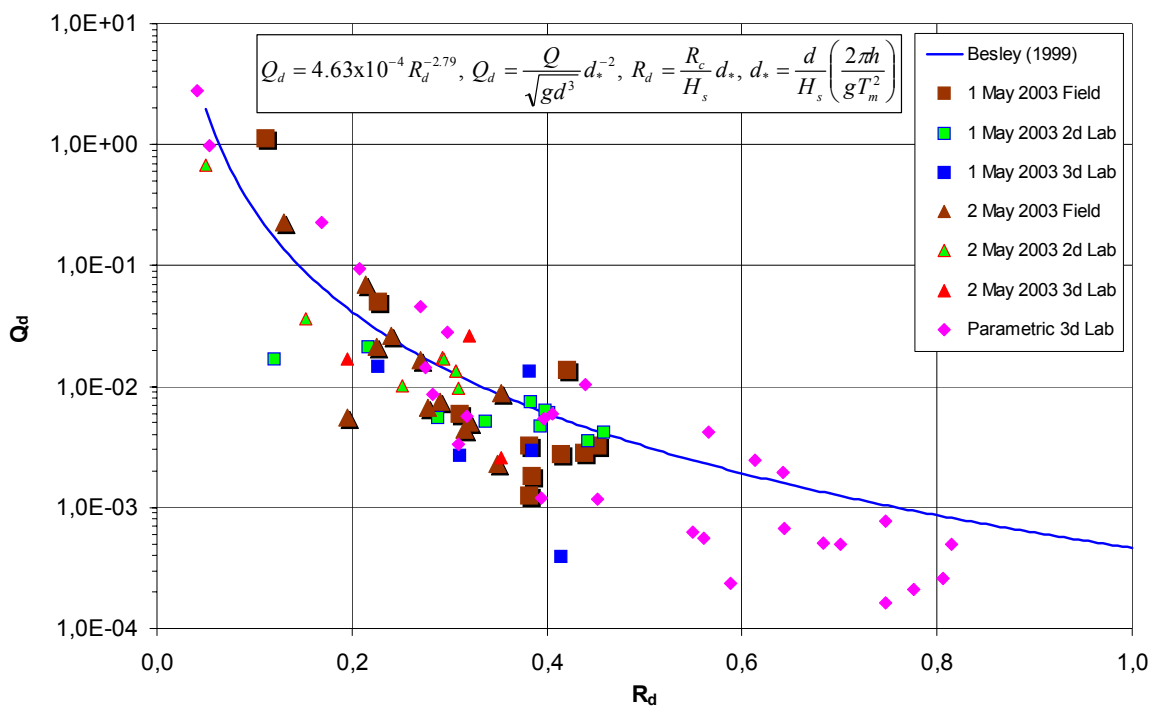


Fig. 9: Prototype results, 2D and 3D test results with comparison to Besley formula

The results in Fig. 9 show a relative good agreement between the Besley curve, most of the data points and the prototype storms. No major differences between field and model data can be observed suggesting that there are only few model (except wind effect) and scale effects.

4.2 Zeebrugge rubble mound breakwater

Some photos taken from videos of two Zeebrugge storms in the field and corresponding model tests in the LWI flume have been plotted in Annex A. One overtopping event is shown in the storm of 7 Oct. 2003 which shows the distribution of overtopping water along the breakwater and some wind effects again. Similar events can be seen in the storm of

8 Febr. 2004 showing that the run-up and overtopping behaviour is similar in the field and the model.

In Fig. 10 all overtopping results at LWI and the prototype results are plotted together as relative mean overtopping rate against the relative freeboard A_c/H_{m0} . The Van der Meer formula for non-breaking waves, Van der Meer (1998), for a roughness factor of $\gamma_f = 0.60$ and $\gamma_f = 0.45$ were also plotted.

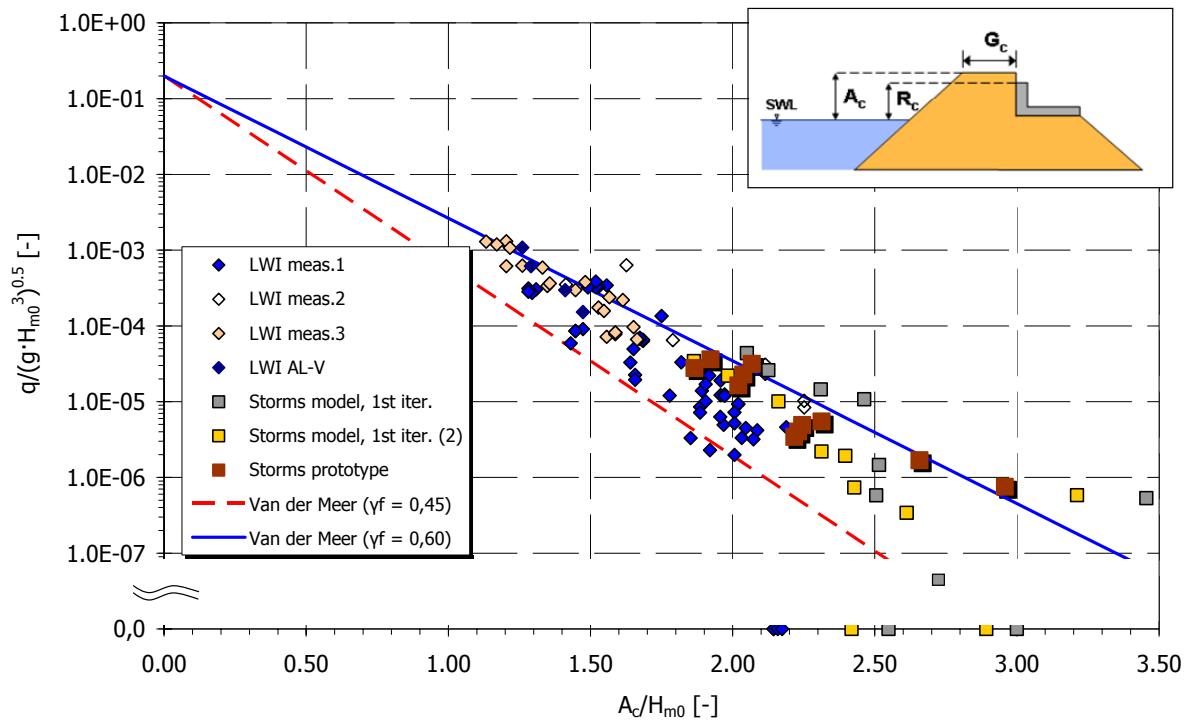


Fig. 10: Relative mean overtopping rates from LWI tests plotted against the relative freeboard with comparison to Van der Meer formula and prototype results¹

The results in Fig. 10 show a relative good agreement between the curves, most of the data points and the prototype storms. However, there is some reasonable scatter in the data and three observations which are of particular importance:

- for higher relative crest freeboard $A_c/H_{m0} > 1,7$ the parametric tests seem to be slightly lower (factor of 2 or 3) than the prototype storms. This is supported by some of the data points which are even zero for $A_c/H_{m0} > 2,0$
- storm reproductions at UPVLC have shown that only one of the three storm events could be reproduced without wind. The other two reproductions had zero overtopping.

¹ Note: to maintain clarity of the diagram only some of the data points from LWI and no tests from UPVLC are shown. Furthermore, no storm data have shown zero wave overtopping rates whereas some of the storm reproductions resulted in zero overtopping

- higher wind speeds in the flume gave considerably higher wave overtopping rates. This cannot be seen from Fig. 10 but has been reported by Kortenhaus et al. (2004b) and González-Escrivá et al. (2004)

Details of differences and reasons for the scatter of the data points are explained in Kortenhaus et al. (2004a).

4.3 Ostia rock breakwater

For the Ostia breakwater the comparison of videos from field and model is more difficult. However, it can be seen that more overtopping occurs in the field rather than in the model. It seems that similar waves cause different behaviour on the slope of the breakwater.

In Fig. 11 all overtopping results at FCFH (3D) and UGent (2D) as well as the prototype results are plotted together as relative mean overtopping rate against the relative freeboard A_c/H_{m0} . The Van der Meer formula for non-breaking waves and a roughness factor of $\gamma_f = 0.60$, $\gamma_f = 0.45$ and $\gamma_f = 0.37$ were also plotted.

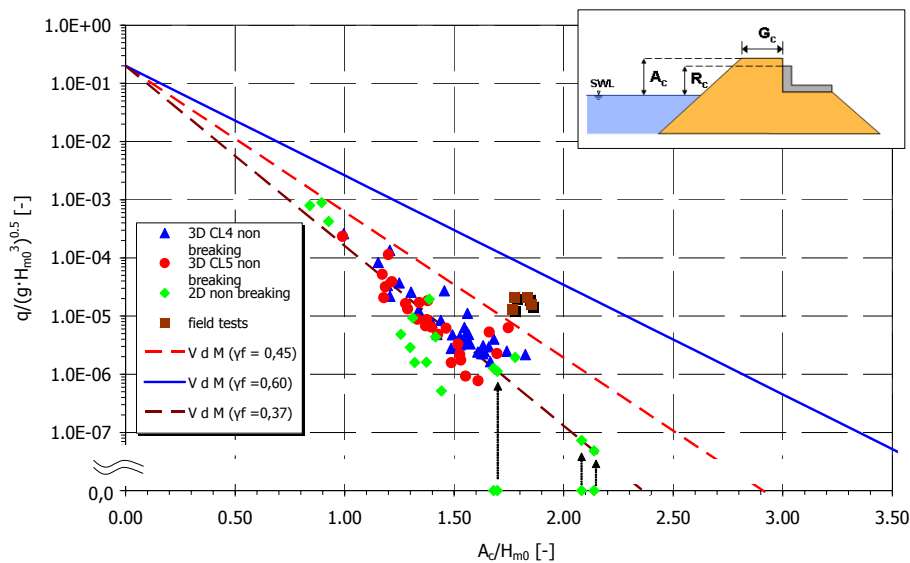


Fig. 11: Relative mean overtopping discharges from FCFH (3D) and UGent (2D) tests plotted against the relative freeboard with comparison to Van der Meer formula and prototype results²

All results in Fig. 11 show a relative good agreement between most of the data points although some scatter can be observed due to variation of some model parameters and influence of wave period. The prototype storm results seem to be higher than the model results (up to a factor of 10).

² Note: almost all data points above a relative crest freeboard of $A_c/H_{m0} > 1.6$ during the model tests were zero whereas prototype data still resulted in overtopping rates

There are four data points in Fig. 11 where the relative mean overtopping rate is zero. No overtopping occurred during the model tests for these data points. It can be assumed, that in the field overtopping could emerge for these ratios A_c/H_{m0} since the measurement accuracy in the flume is not high enough for these small overtopping volumes. In order to calculate prototype values from these data points and account for scale effects, a mean overtopping rate greater than zero has to be determined. Using the Van der Meer formula and a roughness factor of $\gamma_f = 0.37$, all data points of the model tests can be represented as shown in Fig. 11. By means of this curve it is possible to achieve relative mean overtopping discharges for the data points with no overtopping. The arrows in Fig. 11 indicate this procedure.

4.4 Numerical models

This section contains key results of the numerical models in CLASH as far as scale effects are concerned. Details of the models can be taken from the final WP 5 report. Section 4.4.1 summarises the results of the MMU Amazon code whereas section 4.4.2 points out the key findings of the UGent VOF code.

4.4.1 Amazon code

Amazon-SC as described in Qian et al. (2003) is a 2DV, free surface capturing, numerical wave flume developed by Manchester Metropolitan University. The solver is based on the approach taken by Kelecy & Pletcher (1997), together with a novel Cartesian cut cell treatment described by Causon et al. (2001). In order to deal with rubble mound structures the body force term of the Navier-Stokes equations is extended using the method proposed by Huang et al. (2003). The method provides a numerical wave flume which resolves the flow field both in the air and water phases in a time accurate manner, full details of the implementation can be found in section 2 of the final report from WP5 in Ingram et al. (2004) and a summary is provided in section 6.2.1 of the CLASH final report in De Rouck (2004).

In order to examine the effects of applying Froude scaling to overtopping experiments a series of 14 numerical tests has been performed. The model scale structure (Fig. 12), consist of a porous breakwater ($K = 0.56$, $N_w = 35\%$), 0.7 m tall with 1:3 front face, consisting of ten, 10 cm tall steps (to simulate an armour layer). Behind the porous face is a solid, impermeable region, 0.8 m tall. The breakwater was subjected to 0.16 m high regular waves with a period of 2.0 s and overtopping was measured across the crown of the structure. The numerical study allowed instantaneous measurements of both jet velocity and jet thickness to be obtained. In addition to the porous tests the structure has been tested with a completely impermeable configuration. To examine the effects of scale both the permeable and impermeable configurations have been tested with Froude scalings of 1:2, 1:1, 2:1 and 4:1 (the permeability and intrinsic porosity remained constant) and in addition the model scale test has been subjected to 2 s waves of 0.08, 0.10, 0.12 and 0.16 m.

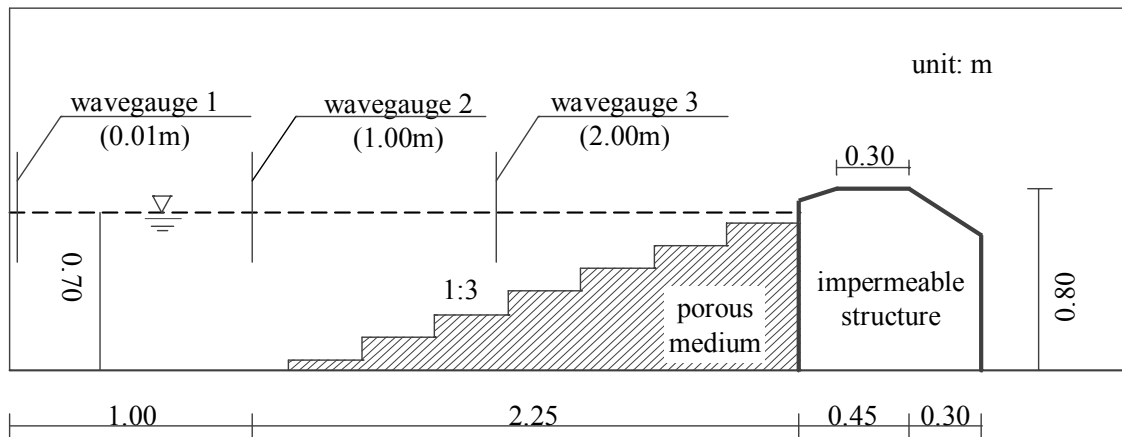


Fig. 12: Computational domain with step porous structure

For each case the instantaneous discharge and the overtopping jet thickness have been measured and the instantaneous jet Reynolds number has been computed. Using a steady state flow over rough surfaces analogy the Darcy-Weisbach friction factor has then been computed and plotted on the Moody diagram. This analysis, following the approach taken by Schulz (1992), is shown in Fig. 13. The results show that for hydraulic independence the Reynolds number should be above 10^5 , requiring tests to be undertaken at scales larger than 4:1 (i.e. in a 100 m wave flume, with a 3.2 m high wall in 2.8 m of water). It should be noted however, that at smaller Reynolds numbers the difference in friction factor is fairly small and the associated discharge velocities (Fig. 14) and overtopping volumes are similar.

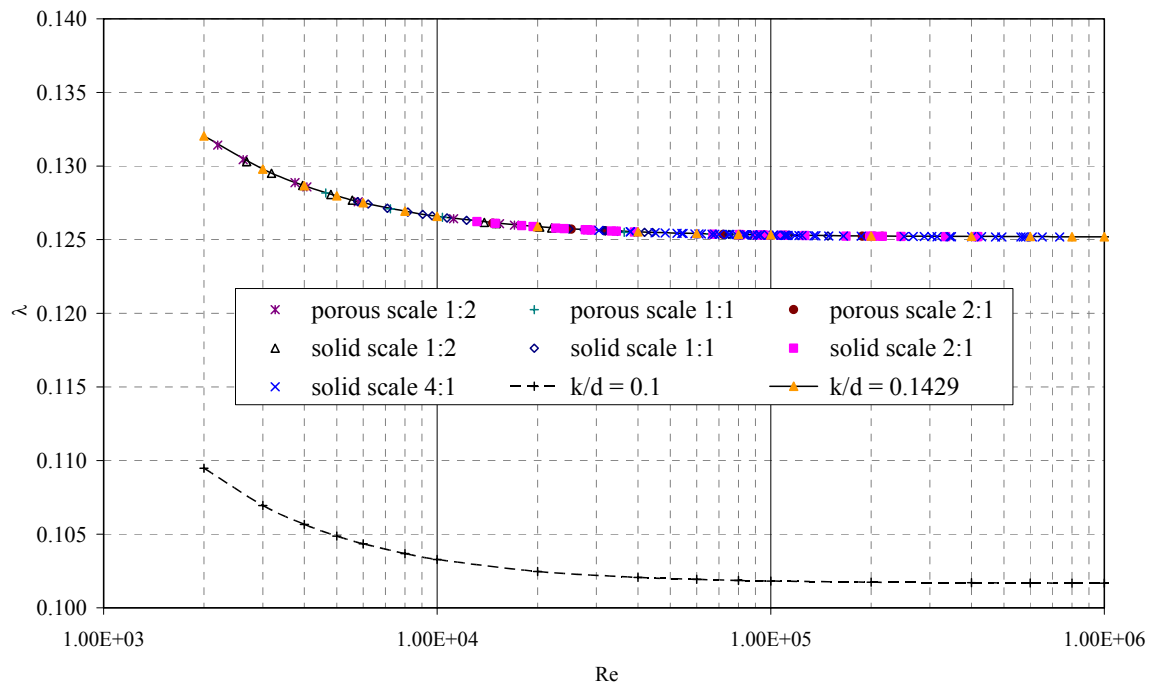


Fig. 13: The Darcy-Weisbach friction factor plotted against Reynolds number

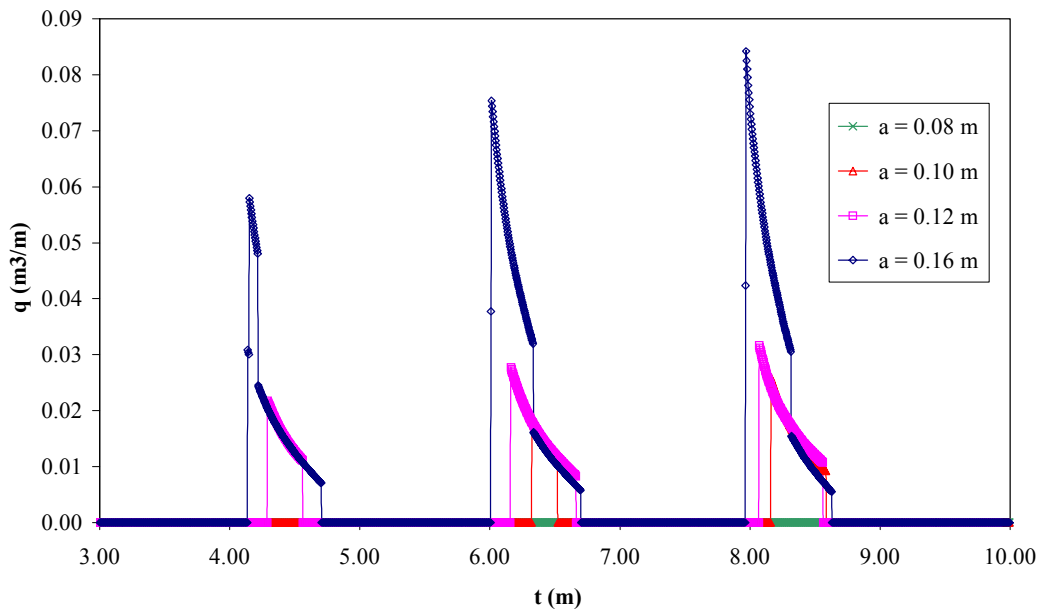


Fig. 14: Instantaneous dimensionless jet velocities (solid breakwater)

In order to assess the effects of varying wave height, the scale 1:1 tests have been repeated with two second period waves with heights of 0.08, 0.10, 0.12 and 0.16 metres. Whilst the 0.08 m waves produced no measurable overtopping the overtopping events produced by the other waves are broadly similar with the volume scaling with the wave height. Fig. 15 shows the instantaneous discharge over the seawall whilst Fig. 16 shows the associated jet velocities. It should be noted that the jump in discharge (observed for the 0.16 m waves) is caused by a plunging jet resulting from wave breaking on the rough structure. Fig. 17 shows the associated instantaneous friction factors which although varying by at most 2.5% during an overtopping event show that, as expected, the variation is larger for larger waves. Similar results are observed on the porous structure.

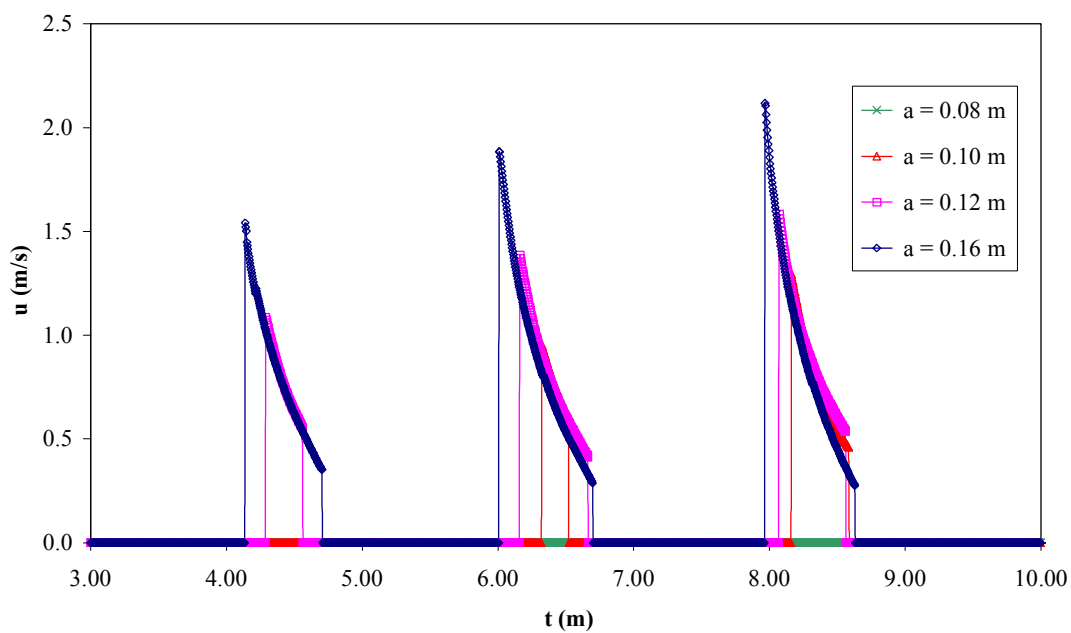


Fig. 15: Instantaneous overtopping volumes measured on the impermeable structure

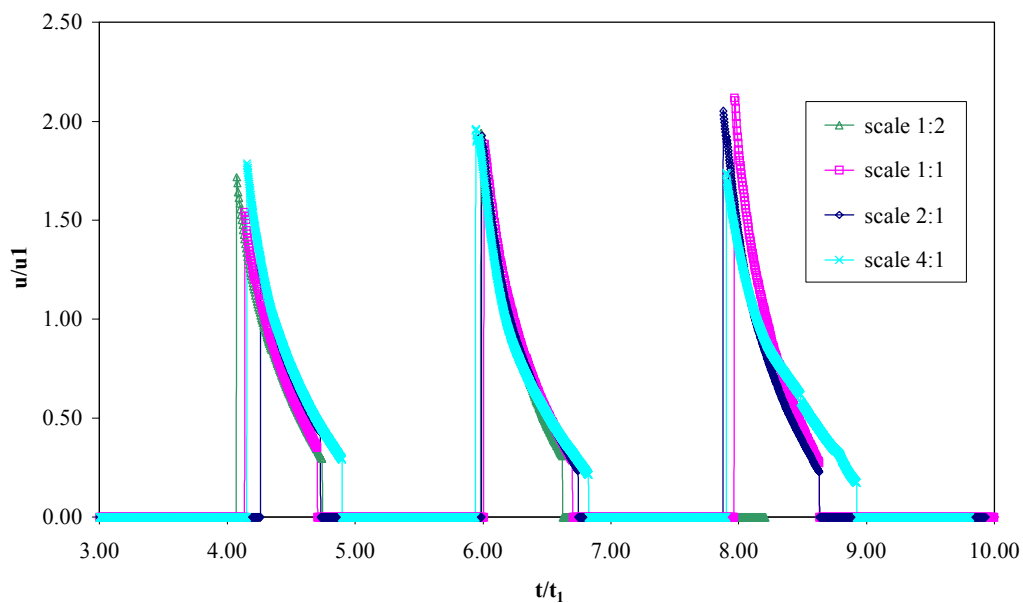


Fig. 16: Instantaneous overtopping jet velocity on the impermeable slope

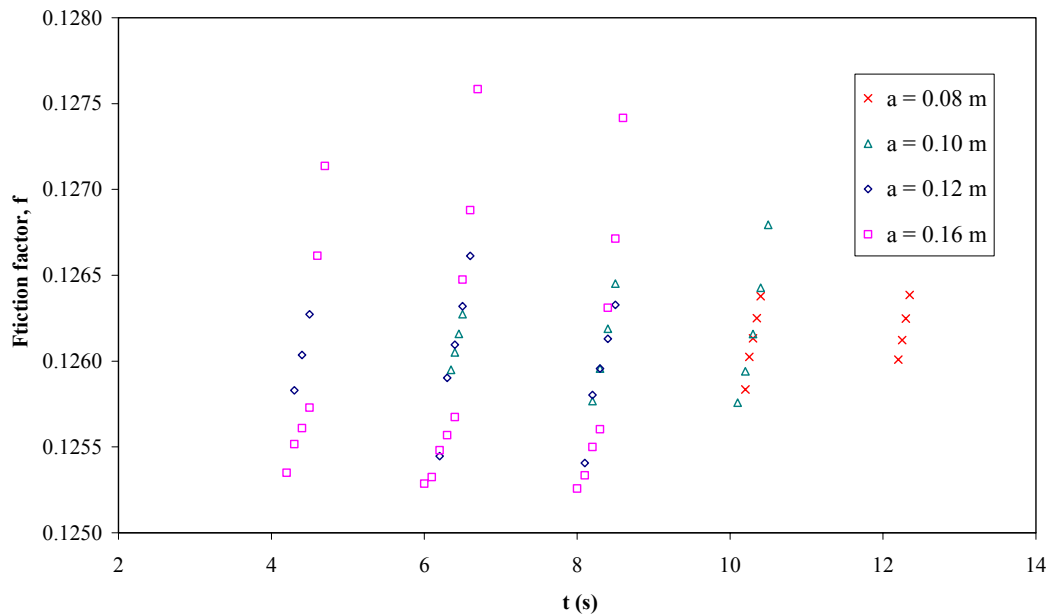


Fig. 17: Instantaneous distribution of the Darcy-Weisbach friction factor for varying wave heights on the impermeable structure

The results indicate that if scaling effects due to friction are to be eliminated then the overtopping jet Reynolds number should be larger than 10^5 , and that this requires (for fairly rough armour units, 4 m nominal diameter at prototype) that the model tests be conducted in a 100 m flume. The simulated effects are much smaller than those observed in the experiments and will include modelling effects. It is likely that using a more sophisticated porosity model would modify these conclusions and the numerical model uses idealised, incompressible, “fresh” water, rather than aerated, compressible, salt water.

4.4.2 Numerical simulation results of 2D wave overtopping at Ostia breakwater

a) Introduction

Numerical simulations of wave overtopping at the Ostia porous rubble mound breakwater have been carried out using the UGent VOFbreak2 code. As a reference case, the 2D 1/20 physical scale model (tested in the UGent wave flume within WP 4) has been used. The physical scale model dimensions have been adopted in the numerical model. Regular wave conditions have been used, identical to the characteristics of the regular wave tests in the physical model. The 1/20 model is used as the reference case for simulating overtopping at the Ostia breakwater, and the numerical model has been used at scales 1/10 and 1/1 subsequently. The scaling is carried out using Froude scaling laws, keeping gravity and viscosity constant for the three different model sizes.

b) Model description

Incident wave conditions are: wave height $H = 0.175$ m, wave period $T = 2.24$ s in water depth (near the paddle) $d = 0.80$ m (and 0.30 m at the toe). The foreshore is modelled according to the foreshore in the physical model. The porous breakwater is composed of a core and an armour layer (identical to the physical model), with material characteristics as given in Tab. 6. The porosity n has been measured in the laboratory from the stones used for constructing the model, the stone diameter d_{50} has the same specifications as the physical model values, and shape factors α , β have been estimated from literature and previous experience.

Tab. 6: Material characteristics for the 1/20 Ostia scale model

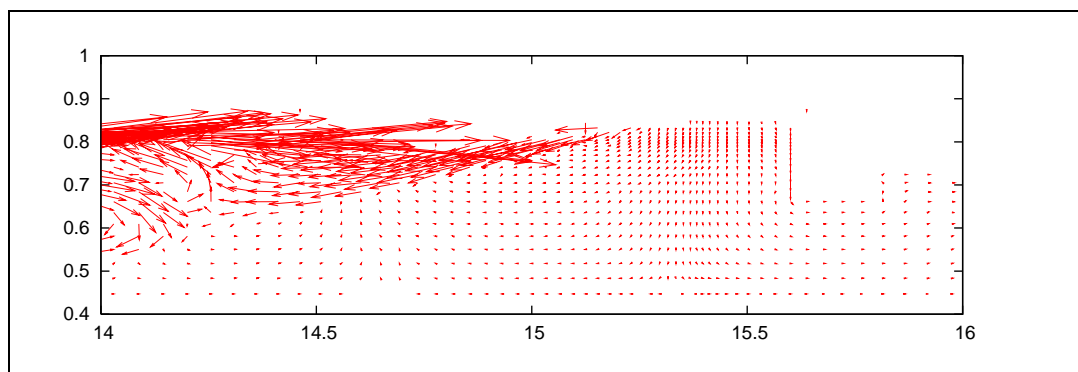
	Core	Armour layer
Porosity n [-]	0.39	0.44
Stone diameter d_{50} [m]	0.025	0.075
Shape factor α [-]	0	0
Shape factor β [-]	2.9	2.7

Using these material characteristics, the Forchheimer coefficients are:

- for the core: $a = 0$, $gb = \beta(1-n)/(n^3d) = 1193$ 1/m;
- for the armour layer: $a = 0$, $gb = \beta(1-n)/(n^3d) = 237$ 1/m.

c) Simulation results

A typical result of the numerical simulation of the free surface configuration for the 1/20 scale model after 5 waves is shown in Fig. 18. The velocity fields calculated at times 18.8, 19.2, 19.6, 20.0 and 20.4 s for the 1/20 scale model are shown in Fig. 18.



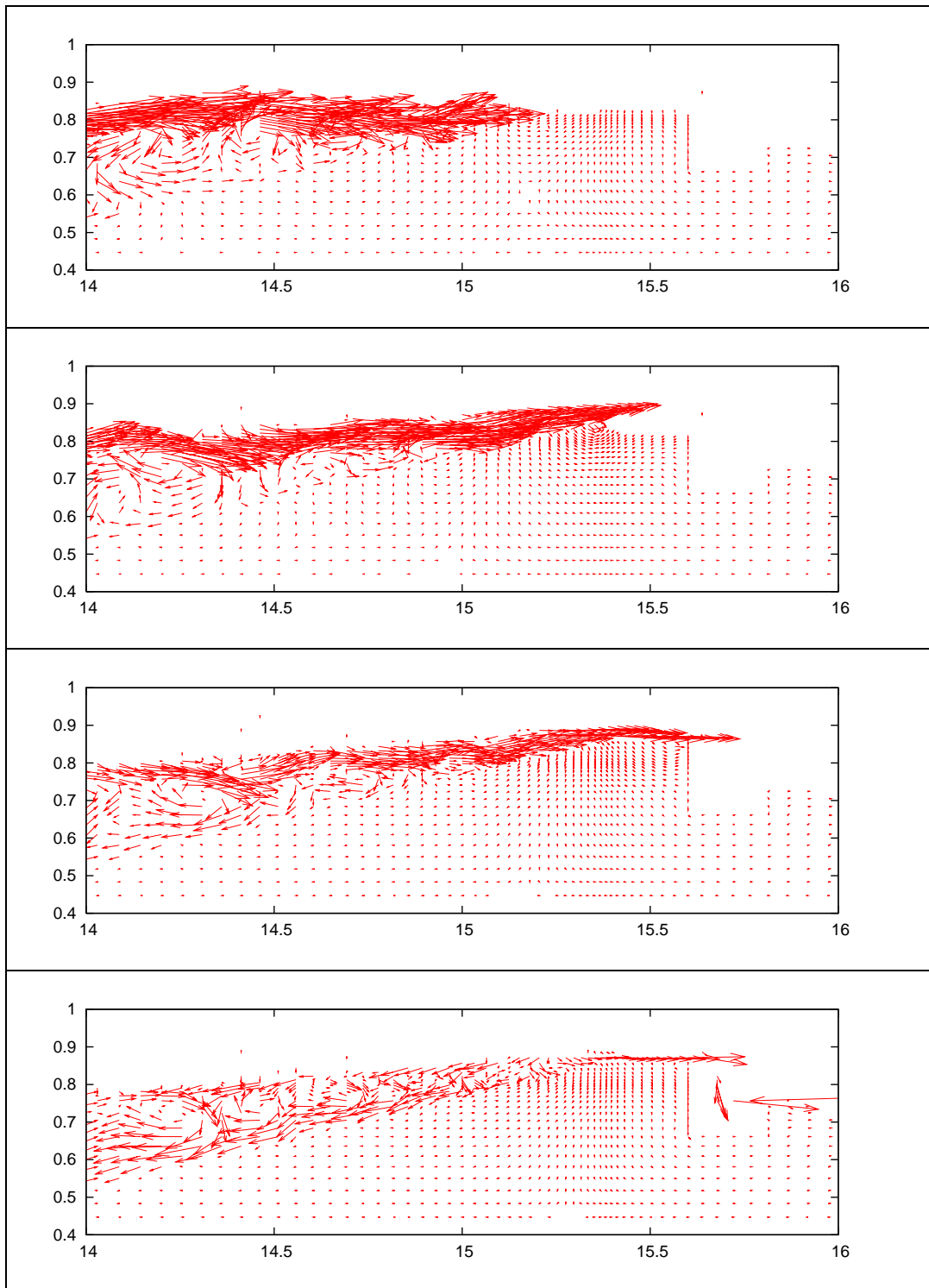


Fig. 18: Simulation results calculated at times 18.8, 19.2, 19.6, 20.0 and 20.4 s for the 1/20 scale model

The results taken from the simulations are the averaged (during one wave period) layer thickness h , the averaged flux (or overtopping rate) q and the averaged Reynolds number Re , taken at two specific locations: on the breakwater slope (at the intersection with the SWL) and on the crest (seaward side). For scaling the 1/20 model to scales 1/10 and 1/1, two approaches

have been used. In the first approach the permeability has been kept constant (stone diameter and β are not scaled, so b is constant), using the second approach, the permeability has been scaled (stone diameter has been scaled). Resulting values are given in Tab. 7. Dimensions are (re-)scaled to the dimensions of the 1/20 model, so layer thicknesses and discharges can be compared easily.

Tab. 7: Averaged (during one wave period) layer thickness h , the averaged flux (or overtopping rate) q and the averaged Reynolds number Re , taken on the breakwater slope (at the intersection with the SWL) and on the crest (seaward side).

Model	On the slope (at SWL)			On the crest		
	h [cm]	q [$\times 10^{-4}$ $m^3/s/m$]	Re [$\times 10^3$]	h [cm]	q [$\times 10^{-4}$ $m^3/s/m$]	Re [$\times 10^3$]
1/20 (lab)	-	-	-	-	6.5	-
1/20 (num)	4.6	91	7	0.5	23.4	1.8
1/10 (constant perm.)	4.2	74	16.1	0.6	10.8	2.3
1/10 (scaled perm.)	5.3	136	29.5	0.9	52.5	11.4
1/1 (constant perm.)	5.0	70	483	0.6	9.2	63.4
1/1 (scaled perm.)	4.5	114	786	0.4	18	124

Compared to the average overtopping rate measured in the physical model tests ($q = 6.5 \times 10^{-4}$), the numerical result is a factor $23.4/6.5 = 3.6$ larger. Since the overtopping waves fill up completely the breakwater, it is assumed that the influence of the shape factors will be small. By increasing the scale to 1/10 and 1/1 and keeping a constant permeability, the numerically calculated overtopping rate on the crest tends to the laboratory value: $9.2/6.5 = 1.4$. By scaling the permeability, larger overtopping rates are obtained.

Reynolds numbers on the slope and on the crest are derived from the results: for the small scale model (1/20) we obtain $Re = 7000$ and 1800 respectively: $Re \sim 0.2 \times 10^4 - 0.7 \times 10^4$. For the prototype (1/1) we obtain $Re \sim 1 \times 10^5 - 5 \times 10^5$.

Resulting Re -values for a second test condition, with wave height $H = 0.175$ m, wave period $T = 2.46$ s in water depth (near the paddle) $d = 0.80$ m (and 0.30 m at the toe) are given in Tab. 8. The same order of magnitude is found, confirming the previous results. Results from simulations using scale 1/1 are not used due to water sloshing against the top boundary of the grid.

Tab. 8: Averaged (during one wave period) Reynolds number Re , taken on the breakwater slope (at the intersection with the SWL) and on the crest (seaward side) for the second test conditions

	On the slope (at SWL)	On the crest
Model	Re [$\times 10^3$]	Re [$\times 10^3$]
1/20 (lab)	-	-
1/20 (num)	2.3	1.1
1/10 (constant perm.)	28	4.4
1/10 (scaled perm.)	39	8.7
1/1 (constant perm.)	-	-
1/1 (scaled perm.)	-	-

A more detailed description of the model and the results is available in a separate report by Constales (2004).

d) Conclusions

Since the core is completely saturated during wave overtopping, porous flow scale effects will be minimal. For flow in the lower part of the run-up wedge (i.e. on the slope), the 1/20 model yields a Reynolds number $Re \approx 0.7 \cdot 10^4$ (close to the critical value $Re_{crit} = 1 \cdot 10^5$ for wave overtopping), and higher Re -values for larger scales, so no scale effects are expected in this region. For flow in the upper part of the run-up wedge (i.e. on the crest), the 1/20 model yields a Reynolds number $Re \approx 0.2 \cdot 10^4$ so scale effects are expected in this region.

4.5 Correction procedures for model and scale effects

Two steps are performed within this section. The first (section 4.5.1) tries to quantify the model effects and uncertainties by applying a Monte-Carlo simulation using the statistical analysis of some of the uncertainties and model effects. The second step (section 4.5.2) summarises the key findings of this report and suggests a simple ‘scaling map’ which helps to identify any possible scale effects and tries to give some simple correction factors.

4.5.1 Monte Carlo simulation for model effects and uncertainties

To obtain information about the magnitude of model effects and uncertainties with respect to wave overtopping Monte Carlo simulations were performed using a standard wave overtopping formula and available information for uncertainties of some parameters as discussed under the previous chapters.

The formula for wave overtopping used within this study has been used widely within CLASH for comparison of prototype and model data, see Van der Meer (1998):

$$\frac{q}{\sqrt{g \cdot H_{m0}^3}} = q_0 \cdot \exp\left(b \frac{R_c}{H_{m0}} \cdot \frac{1}{\gamma_f \cdot \gamma_b \cdot \gamma_\theta}\right) \quad (20)$$

which is equivalent to

$$q = q_0 \cdot \sqrt{g \cdot H_{m0}^3} \exp\left(b \frac{R_c}{H_{m0}} \cdot \frac{1}{\gamma_f \cdot \gamma_b \cdot \gamma_\theta}\right) \quad (21)$$

where H_{m0} is the wave height at the toe of the breakwater in [m], R_c is the relative crest freeboard in [m], q_0 is an empirically determined overtopping rate in [$\text{m}^3/\text{s} \cdot \text{m}$] for zero freeboard and b is also an empirical factor; γ_f is the roughness factor for the outer slope, γ_θ represents the influence of the angle of wave attack and γ_b stands for the influence of the berm width. With regard to the uncertainties of the model tests several factors f_i are introduced extending Eq. (21):

- f_{rep} : factor for the repetition of the tests,
- f_{tray} : factor for the width of the tray,
- f_{spec} : factor for the goodness of fit to the spectrum and

Together with γ_f , γ_b , γ_θ as mentioned above, and a further reduction factor γ_{arm} which accounts for the influence of the armour layer, Eq. (21) reads as follows:

$$q = q_0 \cdot \sqrt{g \cdot H_{m0}^3} \exp\left(b \frac{R_c}{H_{m0}} \cdot \frac{1}{\gamma_f \cdot \gamma_b \cdot \gamma_\theta \cdot \gamma_{\text{arm}}}\right) \cdot f_{\text{rep}} \cdot f_{\text{tray}} \cdot f_{\text{spec}} \quad (22)$$

Eq. (21) is used to perform the Monte Carlo simulations. The values of the input parameters and the uncertainties represented by the mean values, the assumed standard deviations and the distribution types are shown in Tab. 9.

Tab. 9: Uncertainties of input parameters and model tests for Monte Carlo simulations regarding wave overtopping (D = deterministic, N = Normal distribution, LN = Log-Normal distribution)

Basic input parameters		Description	Mean value	Std. dev.	Distr. type
g	[m/s ²]	gravitational acceleration	9.81	-	D
h _k	[m]	height of crown	8.00	0.10	N
MWL	[m]	mean water level	6.75	0.10	LN
γ _f	[-]	roughness factor outer slope	0.55	0.05	N
H _{m0}	[m]	wave height at toe of breakwater	6.20	0.10	N
q ₀	[m ³ /(sm)]	overtopping rate for zero freeboard	0.20	0.10	N
b	[-]	parameter according to van der Meer (1998)	-2.60	0.35	N
γ _{arm.}	[-]	factor for armour layer layout	1.00	0.10	N
Uncertainties of model tests					
f _{rep.}	[-]	factor for repetition of tests	1.00	0.13	N
f _{tray}	[-]	factor for width of tray	1.00	0.23	N
f _{spec}	[-]	factor for the goodness of fit to the spectrum	1.00	0.20	N

A software tool was used to perform 10.000 Monte Carlo simulations for the input values (design values) given in Tab. 9 first. For numerical reasons the logarithm of the overtopping rate $\log(q)$ was used during the calculations. Additional simulations were performed for different values of the crest freeboard R_c varying the mean water level using $MWL = 6.0$ m, 5.0 m and 4.0 m while all other parameters remained unchanged. Furthermore, the wave height was changed to values of $H_{m0} = 2.67$ m, 2.00 m, 1.60 m and 1.17 m with a mean water level of $MWL = 4.0$ m. The results of all simulations are given in Tab. 10 and Fig. 19, respectively. It should be noted that the roughness factor has not been adopted to the data but has been set constant to $\gamma_f = 0.55$ which roughly corresponds to the regression curve of the data points.

Tab. 10: Results of Monte Carlo simulations of wave overtopping formula with variation of MWL and H_{m0}

MWL	6,75	6,00	5,00	4,00	4,00	4,00	4,00	4,00
H_{m0}	6,20	6,20	6,20	6,20	2,67	2,00	1,60	1,17
	[m]							
$\log(q_{mean}) =$	0,479	0,232	-0,109	-0,447	-2,783	-4,014	-5,225	-7,371
$q_{mean} =$	3,014	1,706	0,778	0,357	1,65E-03	9,69E-05	5,95E-06	4,26E-08
$q_{mean}/(g \cdot H_{m0}^3)^{0,5} =$	6,23E-02	3,53E-02	1,61E-02	7,39E-03	1,21E-04	1,09E-05	9,39E-07	1,07E-08
Std. Dev ($\log q_{mean}$) =	0,337	0,354	0,382	0,430	0,714	0,923	1,156	1,618
$\log(q_{mean}) + \text{Std.Dev}$	0,817	0,587	0,273	-0,017	-2,070	-3,091	-4,069	-5,753
$\log(q_{mean}) - \text{Std.Dev}$	0,142	-0,122	-0,491	-0,877	-3,497	-4,936	-6,381	-8,989
$f_+ = (q_{mean} + \text{std.dev})/q_{mean}$	2,18	2,26	2,41	2,69	5,17	8,37	14,32	41,48
$f_- = (q_{mean} - \text{std.dev})/q_{mean}$	0,46	0,44	0,42	0,37	0,19	0,12	0,07	0,02
$f_+ \cdot q_{mean}/(g \cdot H_{m0}^3)^{0,5} =$	1,36E-01	7,98E-02	3,88E-02	1,99E-02	6,24E-04	9,16E-05	1,34E-05	4,46E-07
$f_- \cdot q_{mean}/(g \cdot H_{m0}^3)^{0,5} =$	2,87E-02	1,56E-02	6,68E-03	2,74E-03	2,33E-05	1,31E-06	6,56E-08	2,59E-10

Furthermore, only a limited set of the uncertainties as determined by Kortenhaus et al. (2004a) have been used in the calculations for the different water levels and wave heights. The reason was to determine a minimum spread of the curve which is always present in data obtained from hydraulic model tests, regardless on how accurately the tests were performed. Therefore, the spread of the resulting overtopping curve is smaller than for considering all uncertainties.

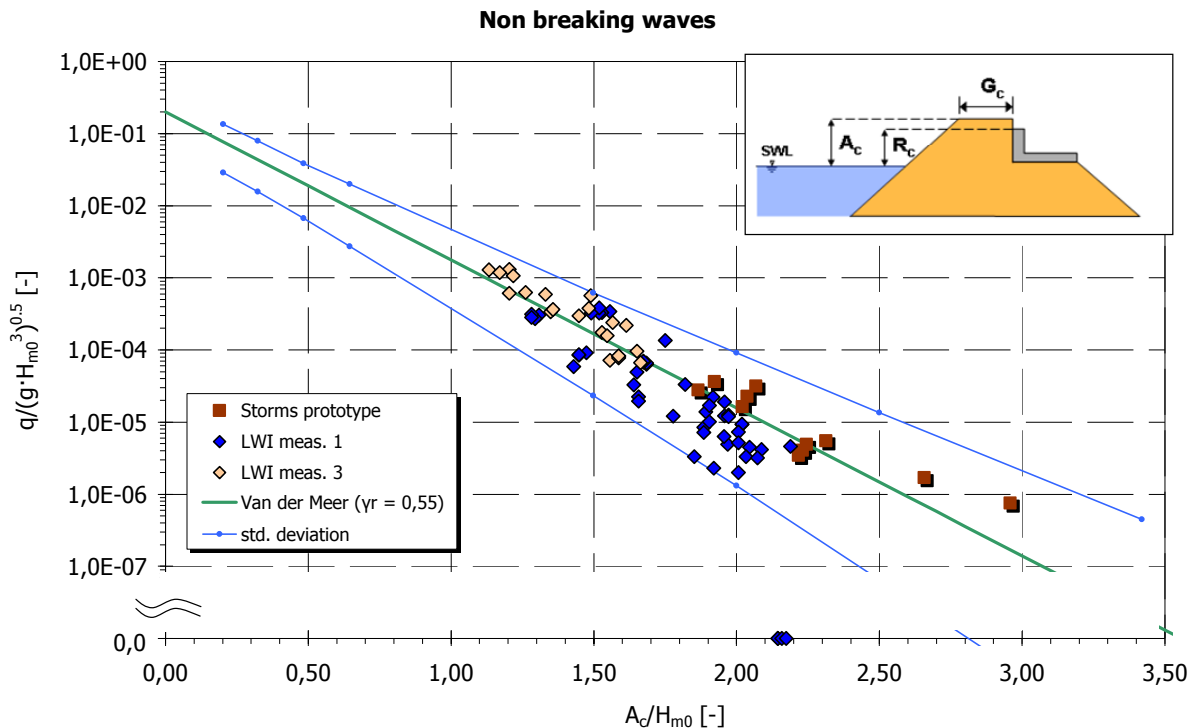


Fig. 19: Results and differences of one standard deviation for wave overtopping formula of the Zeebrugge breakwater

The two lines denoted ‘std. deviation’ in Fig. 19 are giving the deviation from the mean values if just one standard deviation of the resulting overtopping rate is added or subtracted from

the mean values. It can be seen that all data points fall within the two lines so that the scatter of the data might be explained solely by the uncertainties defined above.

4.5.2 Method to account for scale effects

A number of possible reasons for differences between prototype and model scale has been listed in the previous chapters of this report. In section 4.5.1 it has been shown that all measurement uncertainties and model effects may have a considerable effect on wave overtopping so that most data points fall within the differences of one standard deviation of the result although the mean value has not been considered correctly for these calculations. Therefore, scale effects are very difficult to observe since differences in the resulting plots as shown in Fig. 19 may be all due to model effects only.

a) Requirements for scale effects

The theoretical investigations and review of the available literature has shown that differences in wave run-up heights for rough slopes (both permeable and impermeable) have been observed in many cases. Therefore, the wave run-up height should be included in any guidance on how to scale wave overtopping. The following requirements may be derived from the literature and observations in the model and prototype tests:

- scaling effects have only been observed for sloped structures but not for vertical ones;
- the scaling factor must be higher for lower overtopping rates; it even has to work for ‘no overtopping’ measurements in the flume so that some overtopping is measured in prototype;
- roughness of the slope has to be included; critical Reynolds numbers can be defined;
- the core permeability needs to be included where lower permeability in the core creates more run-up on the slope and more overtopping
- wind effects should be included since wind seems to increase wave overtopping rates considerably;

b) Factor resulting from scale effects on wave run-up

The second and third requirement may be fulfilled by a simple approach which is described in the following. Schulz (1992) and others have indicated that the increase of run-up heights from small-scale to large-scale models are in the range of 15%. If this is introduced as an additional ‘roughness’ factor (to be treated in the same way as a traditional roughness factor) to a standard wave overtopping formula it gives:

$$\frac{q_{\text{red}}}{\sqrt{g \cdot H_{m0}^3}} = q_0 \cdot \exp\left(b \frac{R_c}{H_{m0}} \cdot \frac{1}{\gamma_f} \cdot \frac{1}{\gamma_s}\right) \quad (23)$$

where γ_s is the scaling reduction due to scale effects on the seaward slope ($\gamma_s = 1,15$ here). Eq. (23) differs from the standard wave overtopping formula by a factor $1/\gamma_s$ only so that q_{red} can be calculated as $q_{red} = q^{(1/\gamma_s)}$. The relative scaling factor $f_{s,q} = q_{red}/q$ can then be calculated as:

$$f_{s,q} = \frac{q_{red}}{q} = \frac{q^{1/\gamma_s}}{q} \quad (24)$$

where q_{red} is the theoretically reduced overtopping rate as given by Eq. (23). In Fig. 20 the factor given by Eq. (24) is plotted against the wave overtopping discharge using the Zeebrugge parametric tests at LWI from the first test phase. The latter have been scaled up to prototype conditions using Froude law. Each data point is then achieved by performing the following steps:

- derive q for specified tests from measurements;
- scale q up to prototype using Froude law (if q is from model tests);
- calculate the reduced overtopping rate using Eq. (23);
- calculate $f_{s,q}$ for each data point using Eq. (24)

Furthermore, an additional formula for a factor f_{scale_nowind} has been plotted which shows a similar behaviour than Eq. (24) but is closer to the data. This curve can be described by the following equation:

$$f_{scale_nowind} = \begin{cases} f_{scale_nw} & \text{for } \gamma_f \leq 0.7 \\ 5 \cdot (1 - f_{scale_nw}) \cdot \gamma_f + (f_{scale_nw} - 1) \cdot 4.5 + 1 & \text{for } 0.7 < \gamma_f < 0.9 \end{cases} \quad (25)$$

where

$$f_{scale_nw} = \begin{cases} 16.0 & \text{for } q_{SS} < 1 \cdot 10^{-5} \text{ m}^3 / \text{s} \cdot \text{m} \\ 1.0 + 15 \cdot \left(\frac{-\log q_{SS} - 2}{3} \right)^3 & \text{for } q_{SS} < 1 \cdot 10^{-2} \text{ m}^3 / \text{s} \cdot \text{m} \\ 1.0 & \text{for } q_{SS} \geq 1 \cdot 10^{-2} \text{ m}^3 / \text{s} \cdot \text{m} \end{cases} \quad (26)$$

Eq. (26) delivers a scaling factor for really rough structures when $\gamma_f \leq 0.7$. It should be noted that q_{SS} is the wave overtopping rate from small-scale model tests which has been scaled to prototype by using Froude. When $\gamma_f \geq 0.9$ the structure is smooth and the scaling factor will be $f_{scale_nw} = 1.0$. In between both values a linear interpolation can be assumed.

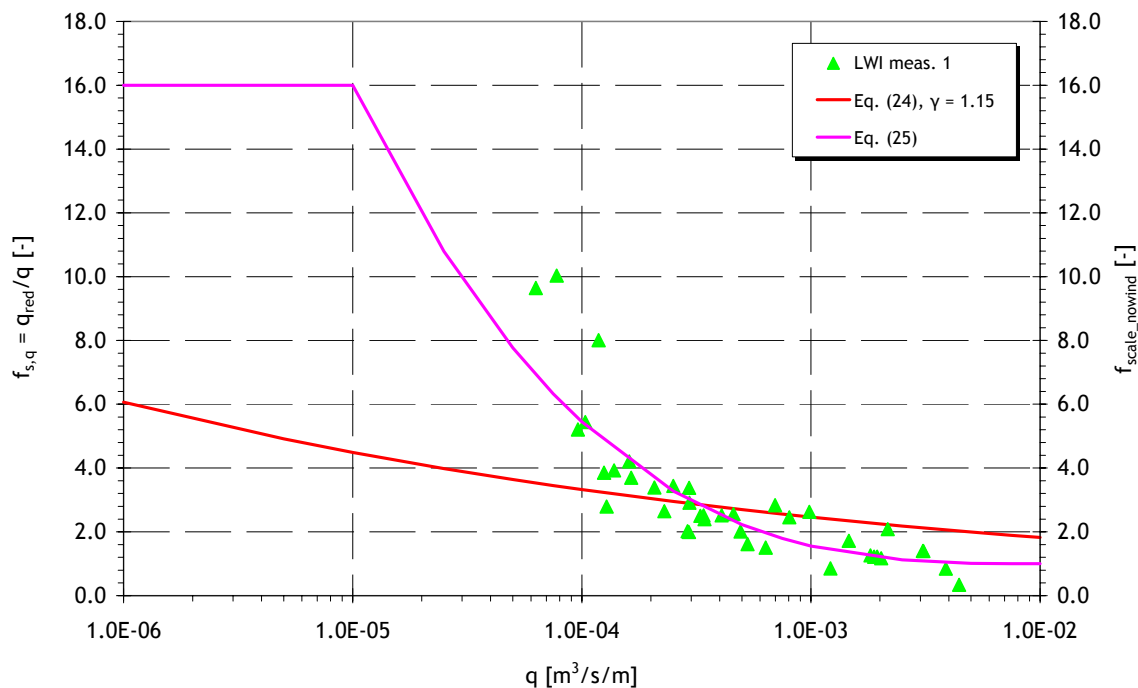


Fig. 20: Reduction of wave overtopping due to reduction of wave run-up on the seaward slope for the Zeebrugge storm data

It can be seen from Fig. 20 that factors may easily go up to one order of magnitude for lower overtopping rates whereas they are still in the same range as without run-up reduction for higher overtopping rates. Since data from comparison between small-scale and large-scale model do not support regions of overtopping ratios lower than $1 \cdot 10^{-5} \text{ m}^3/\text{s} \cdot \text{m}$ the formula will not go up to higher values than a factor of 16.0.

Eq. (24) is determined for a scaling factor which is only valid for rough slopes and no wind effects. The latter can be assumed since comparisons between large-scale and small-scale tests are always referring to tests in either the GWK in Hannover or the Delta flume in De Voorst which both do not include any wind.

Therefore, a method needs to be found which summarises the various influences of scale and wind effects. This method will be discussed in the subsequent section. Since the magnitude of the influence of scaling the core material is not known up to date this influence will be ignored in the following.

c) Factor resulting from wind effect on vertical structures

It is possible to examine the results of de De Waal et al. (1996), Davey (2004) and Pullen & Allsop (2004), as described in section 2.3.2b), by taking advantage of the scaling factor approach developed in section 4.5.2a), Eq. (25). By examining the data it is possible to ascribe the following formula to the transport factor f_{wind} (Fig. 21):

$$f_{wind} = \begin{cases} 4.0 & \text{for } q_{SS} < 1 \cdot 10^{-5} \text{ m}^3 / \text{s} \cdot \text{m} \\ 1.0 + 3 \cdot \left(\frac{-\log q_{SS} - 2}{3} \right)^3 & \text{for } q_{SS} < 1 \cdot 10^{-2} \text{ m}^3 / \text{s} \cdot \text{m} \\ 1.0 & \text{for } q_{SS} \geq 1 \cdot 10^{-2} \text{ m}^3 / \text{s} \cdot \text{m} \end{cases} \quad (27)$$

In this instance the factor 4.0 is not a scaling factor as previously described, but it can be used to make an allowance for the effects of the wind, and also has the advantage of not using a separate technique. It is especially important to make this distinction, because it has been demonstrated by Pullen & Allsop (2004), also described in section 4.1, that there are no scaling effects for vertical and composite vertical structures. Fig. 21 shows that a factor of 4.0 provides a conservative estimate of the effect of the wind with respect to the overtopping discharge rate q .

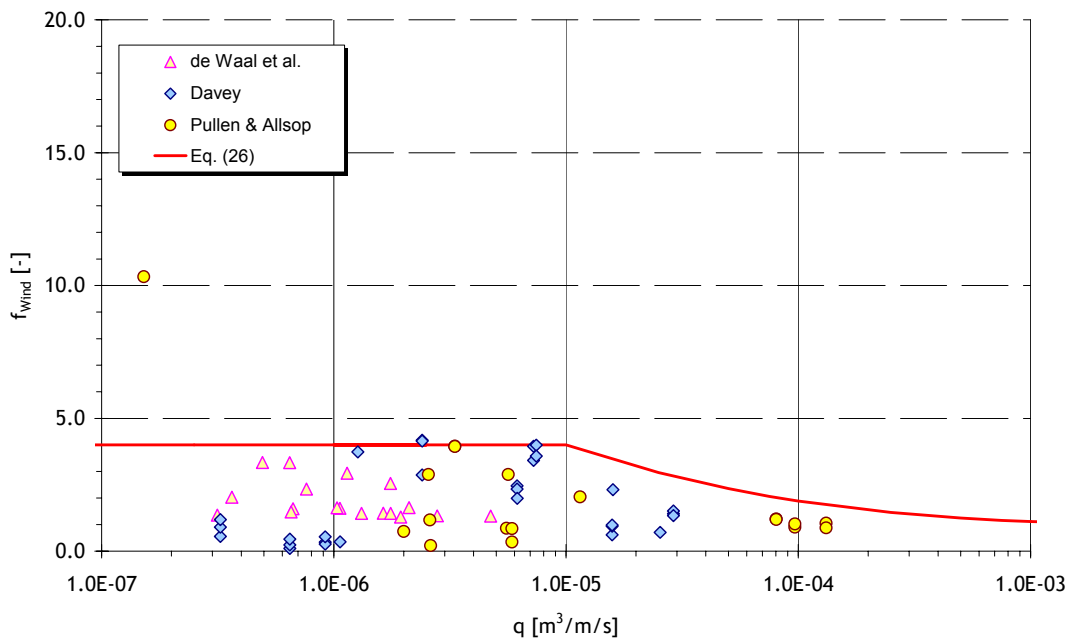


Fig. 21: Discharge rates and the effect of the transport factor f_{Wind}

d) Overall procedure

Input

The final procedure to account for scale effects starts with a mean overtopping rate predicted by small-scale model tests q_{SS} as input. Besides the q_{SS} the following parameters are required:

- wave height H_{m0} at the toe of the structure (output scale³),
- roughness coefficient γ_f for the seaward side of the structure,
- width of the seaward berm B of the structure,
- water depth over the horizontal berm d_h ,
- slope of the structure below the berm $\cot\alpha_d$,
- slope of the structure above the berm $\cot\alpha_u$

For a more detailed description of these parameters see Verhaeghe et al. (2003). The wave height H_{m0} is needed to distinguish between model scale, full-scale or any other scale in between. The roughness coefficient γ_f is needed to distinguish between a smooth and a rough structure whereas all other parameters are needed to select vertical structures or sloped structures.

Output

There are three possible outputs of the procedure which are:

- mean overtopping rate with possible wind effect q_{wind} : wind may play a role for all vertical structures and all smooth (sloping) structures which are believed to have no scale effects
- mean overtopping rate with possible scale and wind effects on rough structures q_{scale_wind} : this output will only be relevant for rough structures and includes both possible scale and wind effects.
- mean overtopping rate with scale effects on rough structures without wind q_{scale_nowind} : this output will only be relevant for rough structures and includes only scale effects. The main interest is to predict wave overtopping rates for large-scale tests without wind.

The prediction method gives all these four mean overtopping discharges q_{SS} , q_{wind} , q_{scale_wind} and q_{scale_nowind} . Differences between these values may give the user a good idea what kind of effect could play a role in his given situation.

Step 1: vertical structure?

Step 1 checks whether the structure is rough sloping or not (Fig. 22). If the structure is vertical or almost vertical continue with ‘Step 4: Procedure wind effect’ If this is not the case go to ‘Step 2: rough structure?’.

Note: To help distinguishing between vertical and non-vertical structures there are two configurations using the input parameters of the CLASH database which indicate a vertical structure. These are:

- if $\cot\alpha_u < 1$ and $\cot\alpha_d < 1$ the structure is vertical or almost vertical.

³ ,output scale’ means that H_{m0} needs to be given in the scale where the final result with respect to wave overtopping rates are needed

- if $\cot \alpha_u < 1$ and $B > 0$ and $d_h > 0$ there is most probably a berm below swl and a vertical structure on top of the berm.

Please note that this parameter distinction cannot be used when parapets are used with the structure. Furthermore, for some complex structures the simple distinction proposed here may fail to give the correct answer.

Step 2: rough structure?

Step 2 checks whether the structure is rough or smooth. If the structure is rough, continue with Step 3: rough sloping structure, if the structure is smooth continue with ‘Step 4: Procedure wind effect’.

Note: The roughness of a structure may be distinguished from the roughness coefficient γ_f of the CLASH database. If γ_f is smaller than 0.9 the structure is considered to be a rough sloping structure otherwise the structure is smooth.

Step 3: rough sloping structure

Within this step the first decision to be made is whether to consider the influence of wind or not. If yes, the factor for scale and wind effects $f_{\text{scale_wind_max}}$ can be calculated as follows:

$$f_{\text{scale_wind_max}} = \begin{cases} 24.0 & \text{for } q_{\text{SS}} < 1 \cdot 10^{-5} \text{ m}^3 / \text{s} \cdot \text{m} \\ 1.0 + 23 \cdot \left(\frac{-\log q_{\text{SS}} - 2}{3} \right)^3 & \text{for } q_{\text{SS}} < 1 \cdot 10^{-2} \text{ m}^3 / \text{s} \cdot \text{m} \\ 1.0 & \text{for } q_{\text{SS}} \geq 1 \cdot 10^{-2} \text{ m}^3 / \text{s} \cdot \text{m} \end{cases} \quad (28)$$

It should be noted that this factor includes both the influence of scale and wind effects, the latter being a model rather than a scale effect. Furthermore, Eq. (25) suggested a maximum factor of 16.0 for scale effects without any wind. Assuming that factors for scale and wind effects should be multiplied to achieve an overall factor, a theoretical factor for wind of 1.5 would be obtained. This is lower than indicated in Eq. (27) for vertical walls, which is believed to be due to the effect of wind for vertical structures being larger than for rough sloping structures.

Eq. (28) delivers a scaling factor for really rough structures when $\gamma_f \leq 0.7$. When $\gamma_f \geq 0.9$ the structure is smooth and the scaling factor will be $f_{\text{scale}} = 1.0$. In between both values a linear interpolation can be assumed so that the scaling factor for rough slopes $f_{\text{scale_wind}}$ can be determined by:

$$f_{\text{scale_wind}} = \begin{cases} f_{\text{scale_wind_max}} & \text{for } \gamma_f \leq 0.7 \\ 5 \cdot \left(1 - f_{\text{scale_wind_max}} \right) \cdot \gamma_f + \left(f_{\text{scale_wind_max}} - 1 \right) \cdot 4.5 + 1 & \text{for } 0.7 < \gamma_f < 0.9 \end{cases} \quad (29)$$

If there is no wind it needs to be decided under which scale the procedure is applied. Therefore, a distinction will be made with respect to the wave height H_{m0} . For wave heights at output scale $H_{m0} < 0.5$ m the factor for scaling is $f_{scale}=1.0$. For all other cases the calculation of f_{scale_nowind} can be performed using Eq. (25). Go to Step 5: Final calculation of mean wave overtopping rate to finalise the procedure.

Step 4: Procedure wind effect

For structures other than rough structures there might be a wind effect. First a decision has to be made whether wind effects are to be considered or not. If not, the factor for the wind-influence is set to $f_{wind} = 1$. If wind effects have to be considered, they can be calculated using Eq. (27).

Finally the factor for wind effects can be applied to the overtopping rate q_{NN} which is performed in “Step 5: Final calculation of mean wave overtopping rate”.

Step 5: Final calculation of mean wave overtopping rate

The final calculation of mean wave overtopping rates should include both a calculation for wind effects and smooth structures and a calculation for scale and wind effects and rough structures as follows:

$$q_{wind} = q_{SS} \cdot f_{wind} \quad (30)$$

$$q_{scale_wind} = q_{SS} \cdot f_{scale_wind} \quad (31)$$

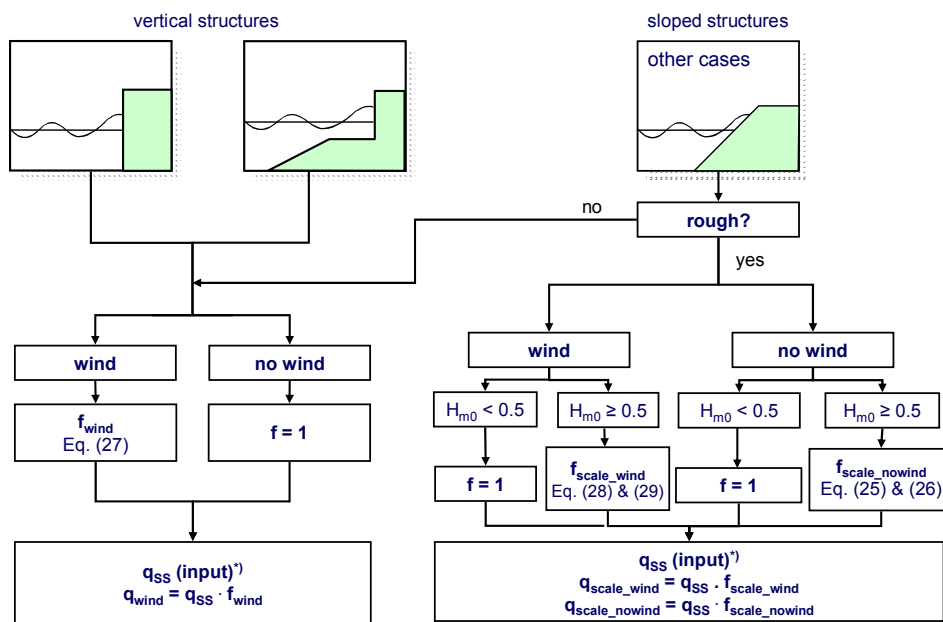
$$q_{scale_nowind} = q_{SS} \cdot f_{scale_nowind} \quad (32)$$

Step 6: Scaling map for coastal structures

The procedure described above is summarised in a simple scaling map for wave overtopping over coastal structures obtained from small-scale model tests (Fig. 22). This map is only needed when

- wave heights H_{m0} for the structure the user is interested in are higher than 0.5 m;
- the user starts from model scale with wave heights $H_{m0} < 0.5$ m

Furthermore, the distinction between vertical and sloped structures as given by the parameters used in Fig. 22 are only valid for structures which do not have parapets or overhanging elements.



*) zero overtopping rates from small-scale model tests can be overcome by the method as described in Fig. 11

Fig. 22: Scaling map for wave overtopping results over coastal structures from small-scale model tests

e) Application of procedure to data from Zeebrugge and Ostia

The aforementioned final procedure to account for scale and wind effects (Fig. 22) has been applied to data from hydraulic model tests for the Zeebrugge and Ostia case. First, the Zeebrugge test case (Fig. 10) has been used. The results are shown in Fig. 23. It should be noted that the correction method for zero data points as described in Chapter 4.3, where the zero value for the mean overtopping rates of four data points was substituted by mean overtopping rates using the Van der Meer formula, was used here as well.

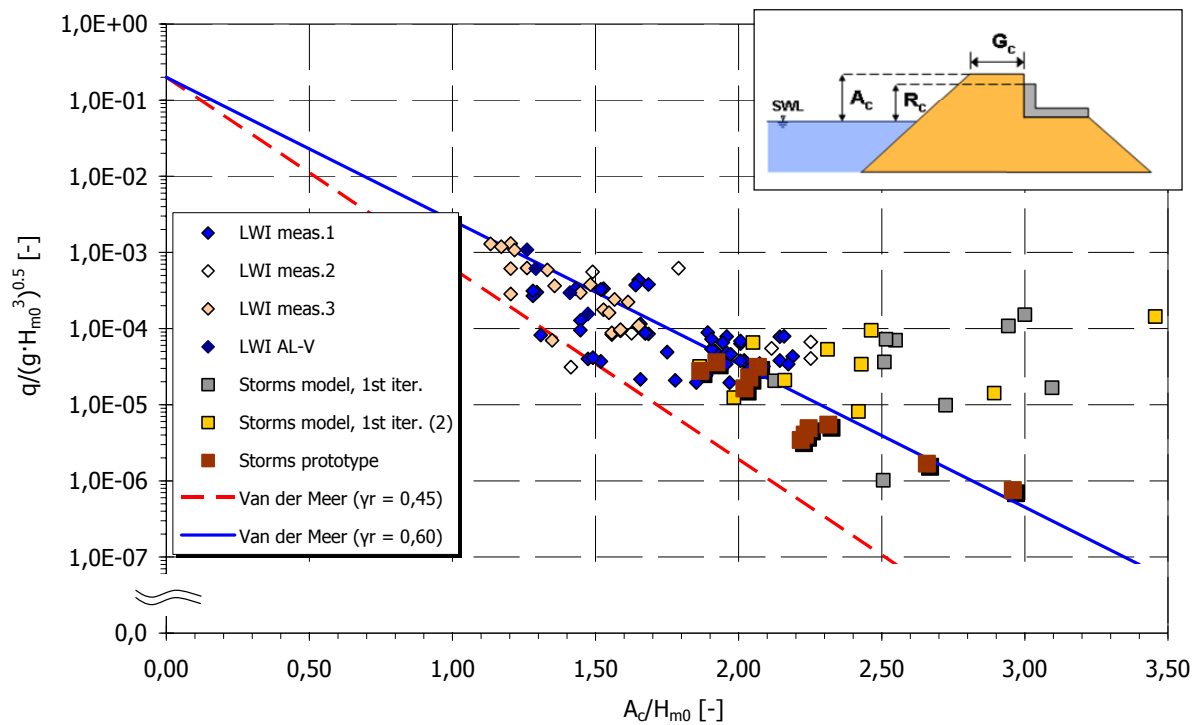


Fig. 23: Results of the application of the parameter map for scaling to the test case of Zeebrugge

It can be seen that compared to the results in Fig. 10 that the increase in wave overtopping rates for the parametric tests such as ‘LWI meas. 1’ and ‘LWI meas. 2’ lead to a better comparison of model and prototype scale data. In general, there is a significant increase of the mean overtopping rate mainly for relative crest freeboards $A_c/H_{m0} \geq 1.7$ where the overtopping rates are up to 30 times higher. Especially the reproductions of storm data during the second phase of the LWI tests are now much higher than the prototype storm data. However, this second phase data have been produced with a different model construction and possibly with a different armour layer setup. This has been shown to have significant influence on the overtopping rates and it is therefore very difficult to compare the different phases of the Zeebrugge tests directly.

In a second step the method was also applied to the data of the Ostia case as shown in Fig. 11. The results of the modifications obtained are given in Fig. 24.

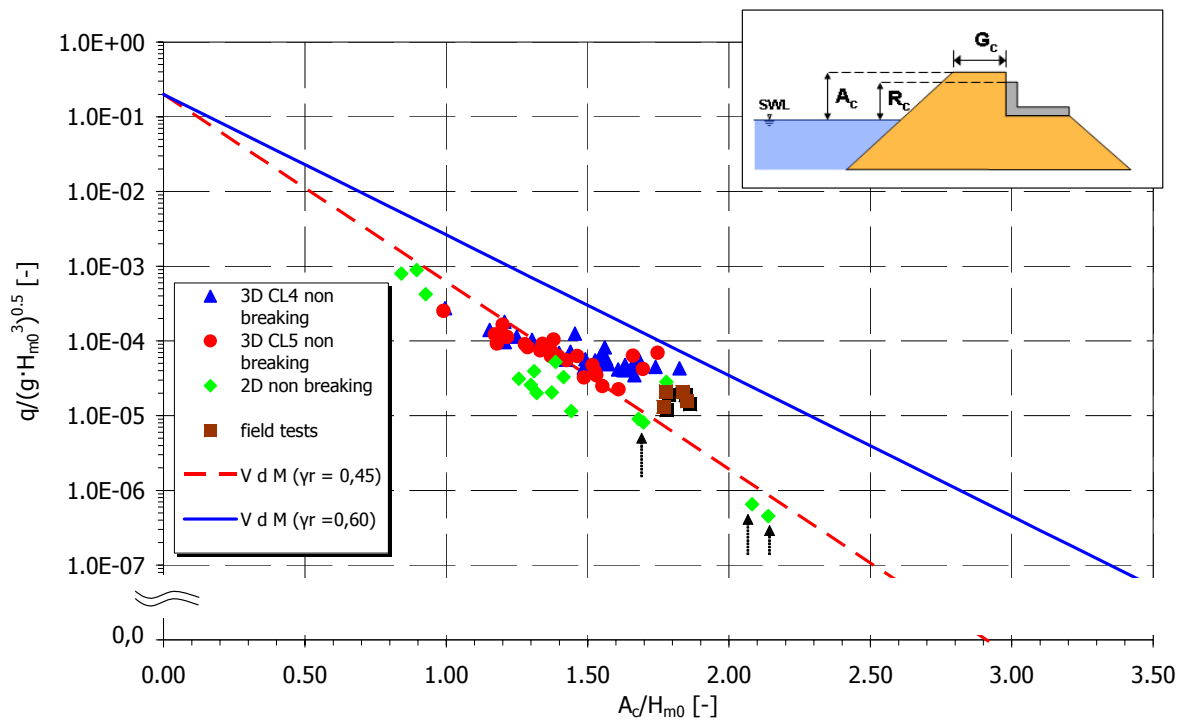


Fig. 24: Results of the application of the parameter map for scaling to the test case of Ostia

The four data points indicated by the arrows in Fig. 24 correlate to the ones mentioned in Chapter 4.3, where the zero value for the mean overtopping rates of four data points was substituted by mean overtopping rates using the Van der Meer formula. The model and prototype data show a much better agreement in Fig. 24 than in Fig. 11 before where especially for the lower overtopping rates a higher increase of all model tests was achieved. Comparing the application for Zeebrugge and Ostia it seems that the developed method gives acceptable results for the cases investigated here.

5 Summary and concluding remarks

CLASH is concentrating on investigations of wave overtopping for different structures in prototype and in laboratory. The model investigations have focussed on wave overtopping and the comparison of overtopping results from small-scale model tests and prototype measurements. Possible differences in the results from small-scale tests and prototype were analysed with respect to measurement accuracy as well as model and scale effects.

This report proposes a methodology to assess the aforementioned effects and to provide the uncertainties and correction factors for quantifying the various influences when performing model tests.

First, the available literature on scale and model effects has been reviewed. It was found that scale effects especially for wave run-up and overtopping have been reported in the past. Many

of these effects have been physically explained by some authors. For some model tests on sea dikes up to 25% higher wave run-ups were observed. Wave overtopping for armour slopes in front of vertical walls in prototype was reported to be up to 10 times higher than in model tests but it is still not clear whether this is due solely to scale effects.

Second, some theoretical considerations were performed to derive critical Weber and Reynolds numbers which should always be exceeded during model tests. It was found that for wave run-up and wave overtopping Weber numbers should not fall below $We_{crit} = 10$ and that water depths should always be larger than 2 cm and wave periods longer than 0,35 s. This is usually the case in all models. Additionally, the overtopping related Reynolds numbers should be larger than $1 \cdot 10^3$ which is also the case for most of the model tests.

Results for all field and model investigations have been plotted for the investigated sites using data from the field and two models of smaller scale. Results have shown that model tests performed for the vertical wall in Samphire Hoe and the steep Zeebrugge rubble mound breakwater do not deviate much from the prototype data points. However, for the flatter slope in Ostia differences between prototype and model have been observed in the order of up to one order of magnitude.

A Monte-Carlo simulation was used to determine the variation which may occur when different measurement uncertainties and scale effects are considered. The results show a large dependency on the magnitude of the overtopping rate itself which was also evident from the observation of the model tests. Differences of a factor of about 5.0 for large overtopping rates and a factor of about 40.0 for low ones are observed.

Finally, a new parameter map for scaling was proposed taking into consideration the aforementioned findings (Fig. 22). The map depends on whether or not the structure is 'rough and sloping' and eventually suggests a scaling predictor. The latter was then applied to the test cases of Zeebrugge and Ostia.

References

- Besley, P. (1999): Wave overtopping of seawalls: design and assessment manual. R&D Technical Report, HR Wallingford, no. W178, Wallingford, U.K., 37 pp., 5 tables (also from: <http://www.environment-agency.gov.uk/commondata/105385/w178.pdf>).
- Biesel, F. (1949): Calcul de l'ammortissement d'une houle dans un liquide visqueux de profondeur finie. *Houille Blanche*, no. 4.
- Broderick, L.L.; Ahrens, J.P. (1982): Rip-rap stability scale effects. U.S. Army Corps of Engineers, CERC Technical Paper, No. 82-3.
- Burcharth, H.F. (2004): On scale effects related to run-up and overtopping for rubble mound structures. CLASH - Crest Level Assessment of Coastal Structures, Workpackage 7, Aalborg, Denmark, 8 pp.

- Burcharth, H.F.; Liu, Z.; Troch, P. (1999): Scaling of core material in rubble mound breakwater model tests. *Proceedings 5th International Conference on Coastal and Port Engineering in Developing Countries (COPEDEC)*, Cape Town, South Africa, pp. 1518-1528.
- Causon, D.; Ingram, D.; Mingham, C.; Pearson, R. (2001): A Cartesian cut cell method for shallow water flows with moving boundaries. *Advances in Water Resources*, vol. 24, pp. 899-911.
- Constales, D. (2004): Numerical simulations of the Ostia breakwater. University of Ghent, Internal report, Ghent, Belgium.
- Dai, Y.B.; Kamel, A.M. (1969): Scale effects tests for rubble mound breakwaters. Research Report U.S. Army Engineer Waterways Experiment Station, H. 69-2, Vicksburg, USA.
- Davey, T. (2004): Overtopping discharge - effect of wind. *MEng project report, School of Engineering & Electronics, University of Edinburgh*, Edinburgh, U.K.
- De Rouck, J. (2004): CLASH final report. CLASH - Crest Level Assessment of Coastal Structures, Ghent, Belgium.
- De Rouck, J.; Troch, P.; Van de Walle, B.; Van der Meer, J.; Van Damme, L.; Medina, J.R.; Willems, M.; Frigaard, P. (2000): Wave run-up on a rubble mound breakwater: prototype measurements versus scale model tests. *Proceedings 27th International Conference Coastal Engineering (ICCE)*, ASCE, Sydney, Australia, 14 pp.
- De Rouck, J.; Troch, P.; Van de Walle, B.; Van Gent, M.R.A.; Van Damme, L.; de Ronde, J.; Frigaard, P.; Murphy, J. (2001): Wave run-up on sloping coastal structures: prototype versus scale model results. In: *ICE (ed.): Breakwaters, coastal structures and coastlines - Proceedings of the International Conference*, Thomas Telford, London, U.K., pp. 232-244.
- De Waal, J.P.; Tonjes, P.; van de Meer, J.W. (1996): Wave overtopping of vertical structures including wind effects. *Proceedings 25th International Conference Coastal Engineering (ICCE)*, ASCE, Volume 2, Orlando, Florida, USA, pp. 2216-2229.
- Delft Hydraulics (1983): Réparation du brise-lames d'Arzew-Djedid. Report Delft Hydraulics Laboratory, Rapport NEDECO-DIB d'Oran, in French.
- Environment Agency (1999): Overtopping of seawalls: design and assessment manual. Report Environment Agency, no. W178, 37 pp., 5 tables.
- Frigaard, P.; Schlütter, F. (1999): Laboratory investigations - methodology. Research Report, MAST III, OPTICREST Project: The optimisation of Crest Level Design of Sloping Coastal Structures Through Prototype Monitoring and Modelling, Aalborg, Denmark, 35 pp.
- Führböter, A. (1986): Model and prototype tests for wave impact and run-up on a uniform 1:4 slope. *Coastal Engineering*, vol. 10, pp. 49-84.
- Funke, E.R.; Mansard, E.P.D. (1979): On the synthesis of realistic sea state in a laboratory flume. NRC Hydraulic Laboratory Technical Report, LTR-Hy-66.
- Gerdes, M.; Kluge, M.; Partensky, H.-W.; Tautenhain, E.; Thoma, M. (1991): Prozeßrechnergestützte Regelung einer Wellenmaschine. *Automatisierungstechnik*, Heft 39, Nr. 5.
- González-Escrivá, J.A.; Garrido, J.; Medina, J.R.; Geeraerts, J. (2004): Laboratory real storm reproduction using wind. *Proceedings 29th International Conference Coastal Engineering (ICCE)*, ASCE, Lisbon, Portugal, 13 pp.

- González-Escrivá, J.A.; Medina, J.R. (2004): Report on generic prediction method. CLASH - Crest Level Assessment of Coastal Structures, Deliverable D11, Workpackage 8, Valencia, Spain, 28 pp.
- González-Escrivá, J.A.; Medina, J.R.; Garrido, J.; De Rouck, J. (2002): Wind effects on runup and overtopping: influence on breakwater crest design. *Proceedings International Conference Coastal Engineering (ICCE)*, ASCE, vol. 28, Volume II, Cardiff, U.K., pp. 2251-2263.
- Huang, C.; Chang, H.; Hwung, H. (2003): Structural permeability effects on the interaction of a solitary wave and a submerged breakwater. *Coastal Engineering*, Elsevier, vol. 49, Amsterdam, The Netherlands, pp. 1-24.
- Hudson, R.Y.; et al. (1979): Coastal hydraulics models. Special Report No. 5, Fort Belvoir, USA.
- Hughes, S.A. (1993): Physical models and laboratory techniques in coastal engineering. Singapore: World Scientific, 568 pp.
- Ingram, D.; Causon, D.; Gao, F.; Mingham, C. (2004): Free surface numerical modelling of wave interactions with coastal structures. CLASH - Crest Level Assessment of Coastal Structures, Workpackage 5, Manchester, Ghent, 53 pp.
- Jamieson, W.W.; Mansard, E.P.D. (1987): An efficient upright wave absorber. In: *ASCE (ed.): Proceedings ASCE Specialty Conference on Coastal Hydrodynamics*, Delaware, USA.
- Jensen, O.J.; Klinting, P. (1983): Evaluation of scale effects in hydraulic models by analysis of laminar and turbulent flows. *Coastal Engineering*, Elsevier, vol. 7, Amsterdam, The Netherlands, pp. 319-329.
- Jonsson, I.G. (1966): Wave boundary layers and friction factors. *Proceedings 1st International Conference Coastal Engineering (ICCE)*, ASCE, Volume 1, Tokyo, Japan, pp. 127-148.
- Kajima, R.; Sakakiyama, T. (1994): Review of works using CRIEPI flume and present work. *Proceedings International Conference on Coastal Dynamics'94*, ASCE, Barcelona, Spain, pp. 614-627.
- Kamphuis, J.W. (1975): Friction factor under oscillatory waves. *Journal of Waterways, Harbors and Coastal Engineering Division*, vol. WWL 101.
- Kececy, F.; Pletcher, R. (1997): The development of a free surface capturing approach for multidimensional free surface flows in closed containers. *Journal of Computational Physics*, vol. 138, pp. 939-980.
- Keulegan, G.H. (1950): Wave motion. *Engineering Hydraulics*: Wiley & Sons, pp. 711-768.
- Klein-Breteler, M.K.; Pilarczyk, K.W. (1996): Stability of artificial roughness elements and run-up reduction. *Proceedings 25th International Conference Coastal Engineering (ICCE)*, ASCE, Volume 2, Orlando, Florida, USA, pp. 1556-1568.
- Klopman, G.; Van der Meer, J.W. (1999): Random wave measurements in front of reflective structures. *Journal of Waterway, Port, Coastal and Ocean Engineering*, vol. 125, pp. 39-45.
- Kolkman, P.A. (1984): Considerations about the accuracy of discharge relations of hydraulic structures and the use of scale models for their calibration. *Symposium on Scale Effects in Modelling Hydraulic Structures*, Esslingen, Germany, pp. 2.1-1-2.1-12.

- Kortenhaus, A.; Medina, J.R.; González-Escrivá, J.A.; Garrido, J. (2004a): Laboratory measurements on the Zeebrugge breakwater. CLASH - Crest Level Assessment of Coastal Structures, Workpackage 4, Final Report, Braunschweig/Valencia, 74 pp., Annexes.
- Kortenhaus, A.; Oumeraci, H. (1999): Scale effects in modelling wave impact loading of coastal structures. In: Evers, K.-U. et al. (eds.): *Proceedings Hydralab Workshop on Experimental Research and Synergy Effects with Mathematical Models*, Hannover, Germany, pp. 285-294.
- Kortenhaus, A.; Oumeraci, H.; Geeraerts, J.; De Rouck, J.; Medina, J.R.; González-Escrivá, J.A. (2004b): Laboratory effects and other uncertainties in wave overtopping measurements. *Proceedings 29th International Conference Coastal Engineering (ICCE)*, ASCE, Lisbon, Portugal, 13 pp.
- Le Mehauté, B. (1976): Similitude in coastal engineering. *Journal of Waterways, Harbors and Coastal Engineering Division*, vol. 102, no. WW3, pp. 317-335.
- Medina, J.R. (1998): Wind effects on runup and breakwater crest design. *Proceedings 26th International Conference Coastal Engineering (ICCE)*, ASCE, Volume 1, Copenhagen, Denmark, pp. 1068-1081.
- Miller, R.L. (1972): The role of surface tension in breaking waves. *Proceedings 13th International Conference Coastal Engineering (ICCE)*, ASCE, Volume I, Vancouver, Canada, pp. 433-449.
- Mol, A. (1983): West breakwaters Sines - study of armour stability. In: *ICE (ed.): Proceedings of the Conference on Coastal Structures and Breakwaters*, Thomas Telford Ltd., London, U.K.
- Müller, D.R. (1995): Auflaufen und Überschwappen von Impulswellen an Talsperren. *Mitteilungen der Versuchsanstalt für Wasserbau, Hydrologie und Glaziologie der ETH Zürich*, Band 137, Zürich, Switzerland, S. 1-201.
- Murphy, J. (1999): Wave run-up measurement techniques. OPTICREST research report on Subtask 3.2.
- Oumeraci, H. (1984): Scale effects in coastal hydraulic models. *Symposium on Scale Effects in Modelling Hydraulic Structures*, Esslingen, Germany, pp. 7.10-1-7.10-7.
- Oumeraci, H. (1998): Möglichkeiten und Grenzen von physikalischen Modellen im Küstenwasserbau. *100 Jahre Dresden*, Dresden, Germany, 21 S.; 2 Abb.
- Oumeraci, H. (1999a): Physical modelling, field measurements and numerical modelling in coastal engineering: synergy or competition? *2nd German-Chinese Joint Seminar on Recent Developments in Coastal Engineering - Sustainable Development in the Coastal Zone*, Tainan, Taiwan, pp. 513-537.
- Oumeraci, H. (1999b): Strengths and limitations of physical modelling in coastal engineering - synergy effects with numerical modelling and field measurements. In: Evers, K.-U. et al. (eds.): *Keynote Address, Proceedings Hydralab Workshop on Experimental Research and Synergy Effects with Mathematical Models, Keynote lecture*, Hannover, Germany, pp. 7-38.
- Oumeraci, H.; Kortenhaus, A.; Allsop, N.W.H.; De Groot, M.B.; Crouch, R.S.; Vrijling, J.K.; Voortman, H.G. (2001): Probabilistic design tools for vertical breakwaters. Rotterdam, The Netherlands: Balkema, 392 pp.
- Pearson, J.; Bruce, T.; Allsop, W.; Gironella, X. (2002): Violent wave overtopping - measurements at large and small scale. *Proceedings 28th International Conference Coastal Engineering (ICCE)*, ASCE, Volume II, Cardiff, UK, pp. 2227-2238.

- Popov, I.J.; Ryabych, V.-M. (1971): Volnovoe davlenie na otkosy zemljanich gidrotechnicheskikh sooruzvenij. *Izbestia VNIIG*, vol. 97, Leningrad, Russia, pp. 49-62.
- Pullen, T.; Allsop, N.W.H. (2004): Clash workpackage 4 - Samphire Hoe physical model studies. CLASH - Crest Level Assessment of Coastal Structures, no. TR 147, Workpackage 4, Wallingford, U.K.
- Qian, L.; Causon, D.; Ingram, D.; Mingham, C. (2003): A Cartesian cut cell two fluid solver for hydraulic flow problems. *Journal of Hydraulic Engineering*, ASCE, vol. 129, no. 9, pp. 688-696.
- Sakakiyama, T.; Kajima, R. (1998): Scale effects on wave overtopping of seawall covered with armour units. *Proceedings 26th International Conference Coastal Engineering (ICCE)*, Copenhagen, Denmark, 2 pp.
- Sand, S.E. (1985): Influence of wave board type on bounded long waves. *Journal of Hydraulic Research*, vol. 23, no. 2.
- Schulz, K.-P. (1992): Maßstabeffekte beim Wellenaufwurf auf glatten und rauhen Böschungen. *Mitteilungen Leichtweiß-Institut für Wasserbau der Technischen Universität Braunschweig*, Heft 120, Braunschweig, Germany, S. 135-244.
- Schüttrumpf, H. (2001): Wellenüberlaufströmung bei Seedeichen - experimentelle und theoretische Untersuchungen. Fachbereich Bauingenieurwesen, Technische Universität Braunschweig. Ph.D. thesis, *Mitteilungen Leichtweiß-Institut für Wasserbau der Technischen Universität*, Braunschweig, Germany, S. 1-124.
- Sharp, J.J.; Khader, M.H.A. (1984): Scale effects in harbour models involving permeable rubble mound structures. *Symposium on Scale Effects in Modelling Hydraulic Structures*, Esslingen, Germany, pp. 7.12-1-7.12-5.
- SPM (1984): Shore protection manual, vol. II, Chapters 6 through 8; appendices A through D. Vicksburg, Mississippi, USA: 800 pp.
- Torum, A.; Mathiesen, B.; Escutia, R. (1977): Scale and model effects in breakwater model tests. *Port and Ocean Engineering under Arctic Conditions (POAC)*, Norway.
- Van der Meer, J.W. (1998): Wave run-up and overtopping. In: *Pilarczyk, K.W. (ed.): Dikes and revetments*, Rotterdam/Brookfield: A.A. Balkema, pp. 145-160.
- Van der Meer, J.W. (2004): Influence of roughness on wave run-up: scale effect? CLASH - Crest Level Assessment of Coastal Structures, Workpackage 7, 3 pp.
- Verhaeghe, H.; Van der Meer, J.W.; Steendam, G.J. (2003): Report: database on wave overtopping at coastal structures. CLASH - Crest Level Assessment of Coastal Structures, Workpackage 2, Delft, The Netherlands, 34 pp., 2 Appendices.
- Ward, D.L.; Widner, C.G.; Zhang, J.; Edge, B.L. (1994): Wind effects on runup and overtopping. *Proceedings 24th International Conference Coastal Engineering (ICCE)*, ASCE, Volume 2, Kobe, Japan, pp. 1687-1699.
- Ward, D.L.; Zhang, J.; Widner, C.G.; Cinotto, C.M. (1996): Wind effects on runup and overtopping of coastal structures. *Proceedings 25th International Conference Coastal Engineering (ICCE)*, ASCE, Volume 2, Orlando, Florida, USA, pp. 2206-2215.
- Weggel, J.R. (1976): Wave overtopping equation. *Proceedings 15th International Conference Coastal Engineering (ICCE)*, ASCE, Volume 3, Honolulu, Hawaii, USA, pp. 2737-2755.